



Air Force Research Laboratory



ELECTRICAL CONDUCTIVITY AND EQUATION OF STATE FROM MEASUREMENTS OF A TAMPED ELECTRICALLY EXPLODING FOIL



Edward L. Ruden, David J. Amdahl, Rufus H. Cooksey,
Matthew T. Domonkos, and Paul R. Robinson
AFRL, Directed Energy Directorate

Francis T. Analla, Darwin J. Brown,
and Mark R. Kostora
Science Applications International Corporation

J. Frank Camacho
NumerEx, LLC

Integrity ★ Service ★ Excellence



Abstract



Results are presented for an experiment that produces and diagnoses dynamic surface conditions of homogeneous warm dense matter (WDM) to infer intrinsic bulk properties such as density, pressure, temperature, specific energy, electrical conductivity, and emissivity in the ranges of up to few eV and down to 0.1 solid density – typical of those encountered in single shot pulsed power device electrodes. The goal is to validate ab initio models of matter encountered for predictive modeling of such devices. In the test whose results are presented here, the WDM is produced by Ohmically heating and exploding an 80 μm Al foil placed between two fused quartz tampers by the discharge of a 36 μF capacitor bank charged to 30.1 kV and discharged in 2.55 μs to a peak load current of 460 kA. Measurements are presented from two division of amplitude polarimeters which operate at 532 nm and 1064 nm, a complementary pyrometer which measures the spectral radiance ratio at those wavelengths, a long-range 660 nm photonic Doppler velocimeter, and a B-dot probe array from which the aforementioned intrinsic properties may be inferred. Available results are compared to a 3-D MHD ALEGRA simulation of the full dynamic load and return conductor geometry. The simulation assumes a two-loop external coupled circuit with lumped elements experimentally characterized by current measurements from complementary shorted and exploding foil capacitor bank discharge tests.

* Work supported by AFOSR LRIR 11RD01COR 3001HK04



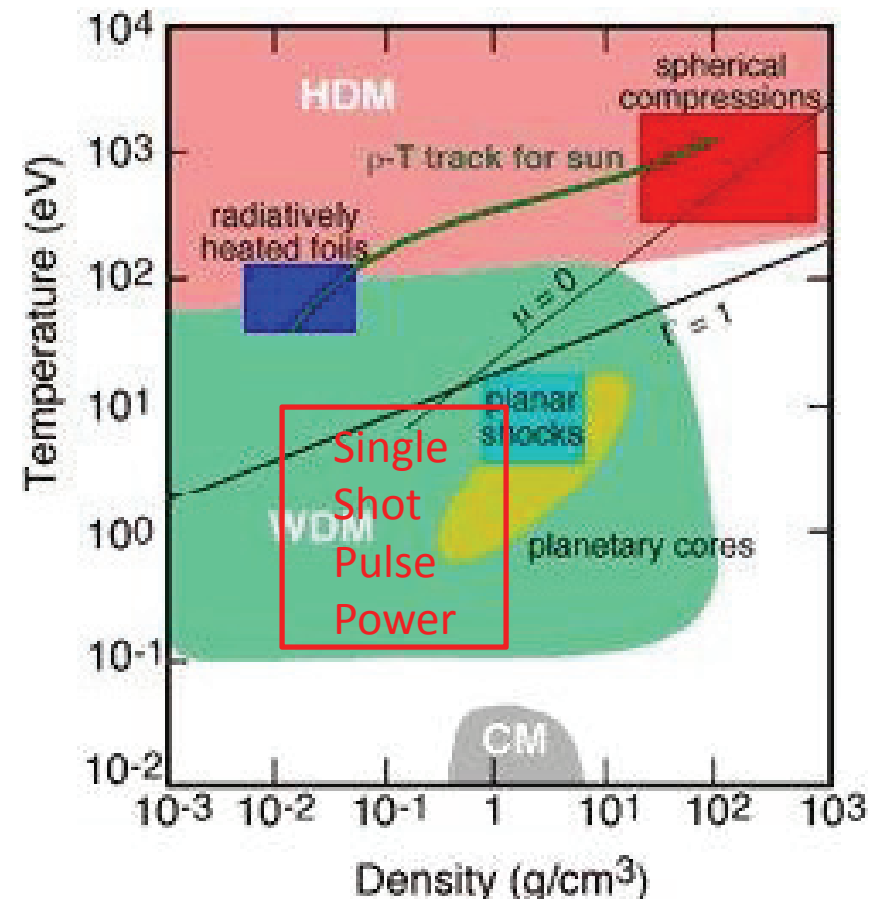
Electrical Conductivity and Equation of State Experiment Research Objectives



GENERAL: Provide basis for 3-D modeling of transition from room T to plasma for full (cold start) predictive capability.

SPECIFIC:

- Produce *homogeneous* Warm Dense Matter from Ohmically exploded tamped foils in the regime characteristic of single-shot pulsed power.
- Diagnose dynamic *surface* conditions to determine *intrinsic* properties.
- Model *intrinsic properties* with quantum many body simulations.
- Model *dynamics* with 3-D MHD simulation.
- Validate theoretical *ab initio* models of matter encountered in single-shot pulsed power devices.
- Develop capability to perform 3-D MHD via ALEGRA.
- Develop in-house capability for *ab initio* simulations.
- Develop powerful optical diagnostic capability (pyrometry, polarimetry, PDV interferometry).

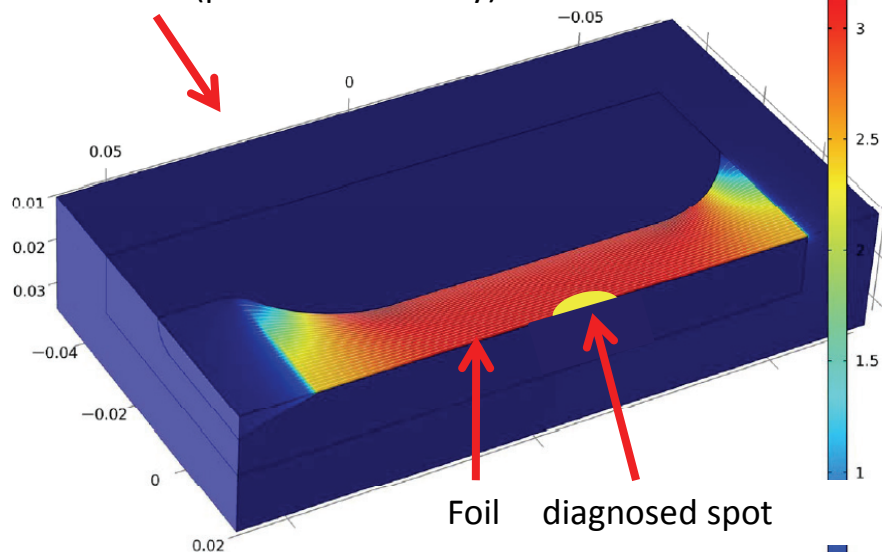




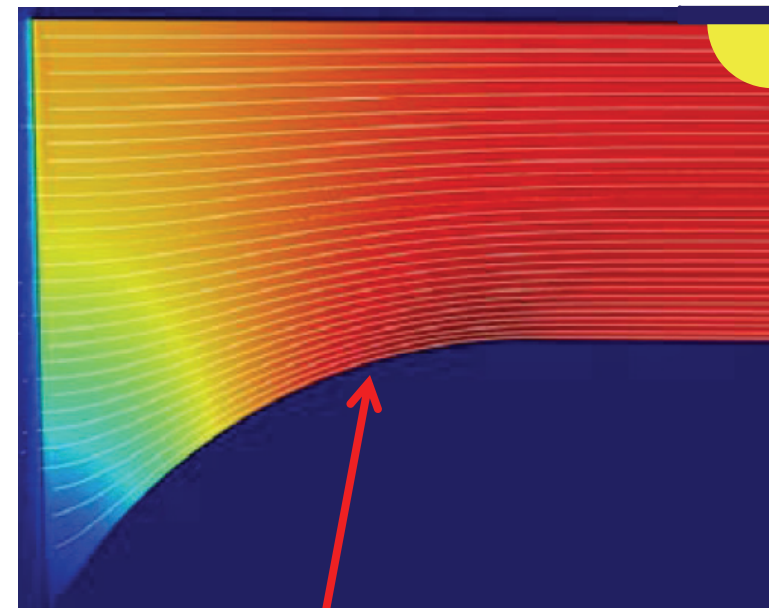
Technical Approach



Return conductor (problem boundary)



freq(4)=10e5 Surface: Current density norm (A/m²) Streamline: Current density

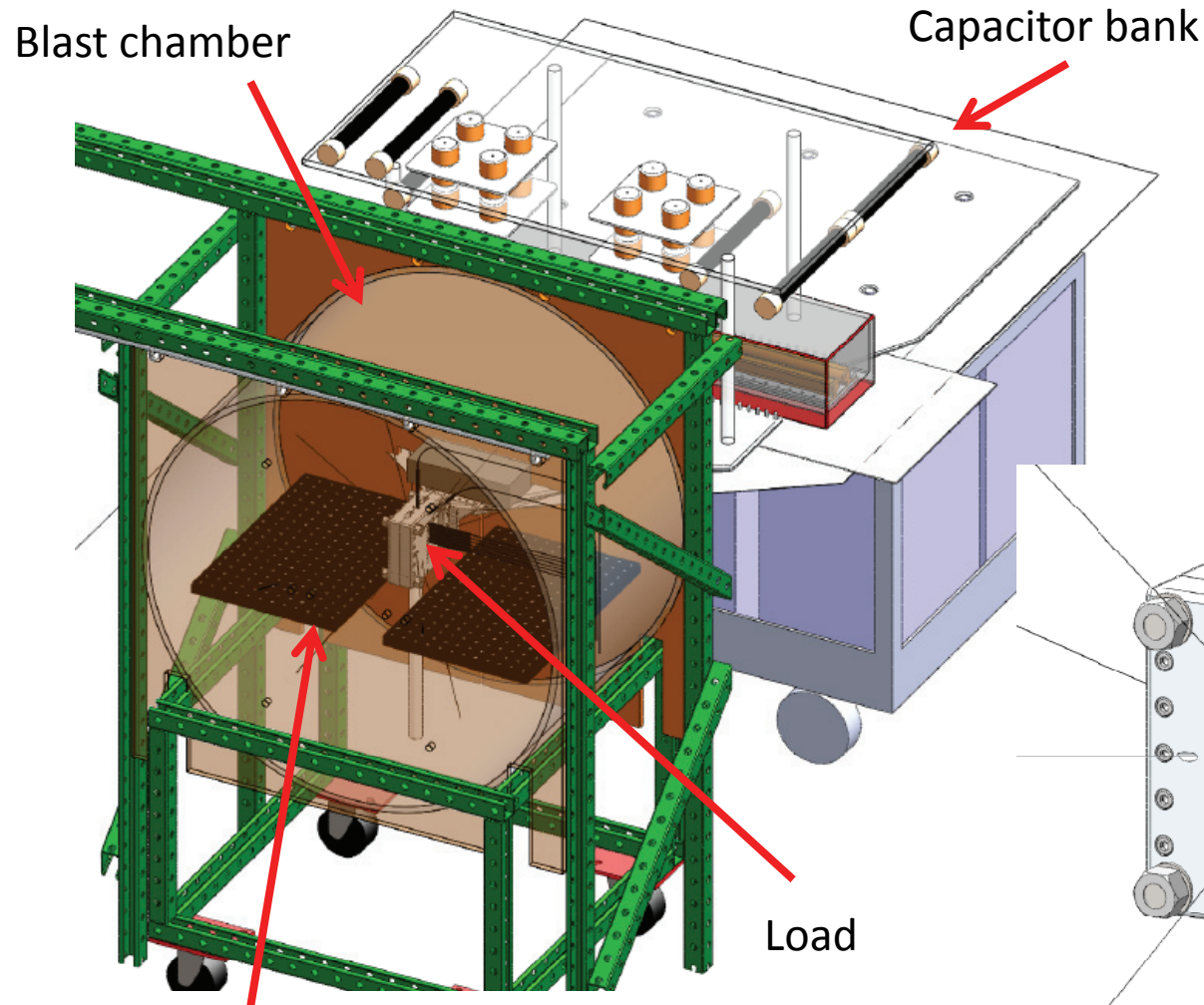


Current density contours from external bank (COMSOL sim)

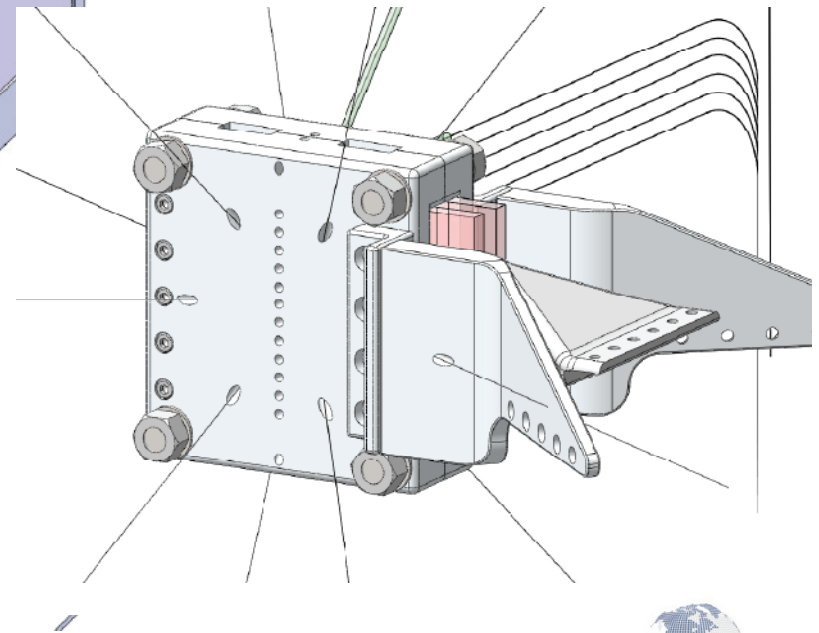
A 30 kJ capacitor bank drives high current density through a fused silica tamped Al foil, which Ohmically explodes, but remains in regime compatible with homogeneous conditions. External compression to be applied in Phase II.



Technical Approach



Overall Assembly Drawing



Optical breadboards flank load for steering mirrors only (diagnostics outside)

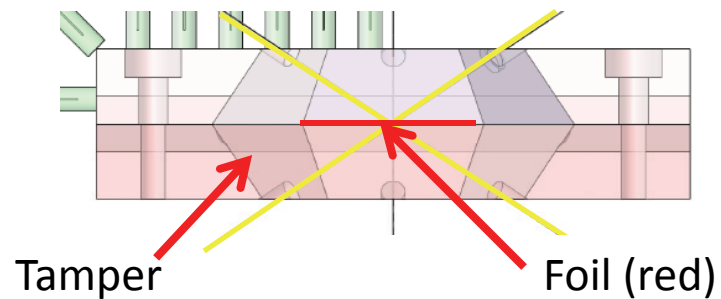
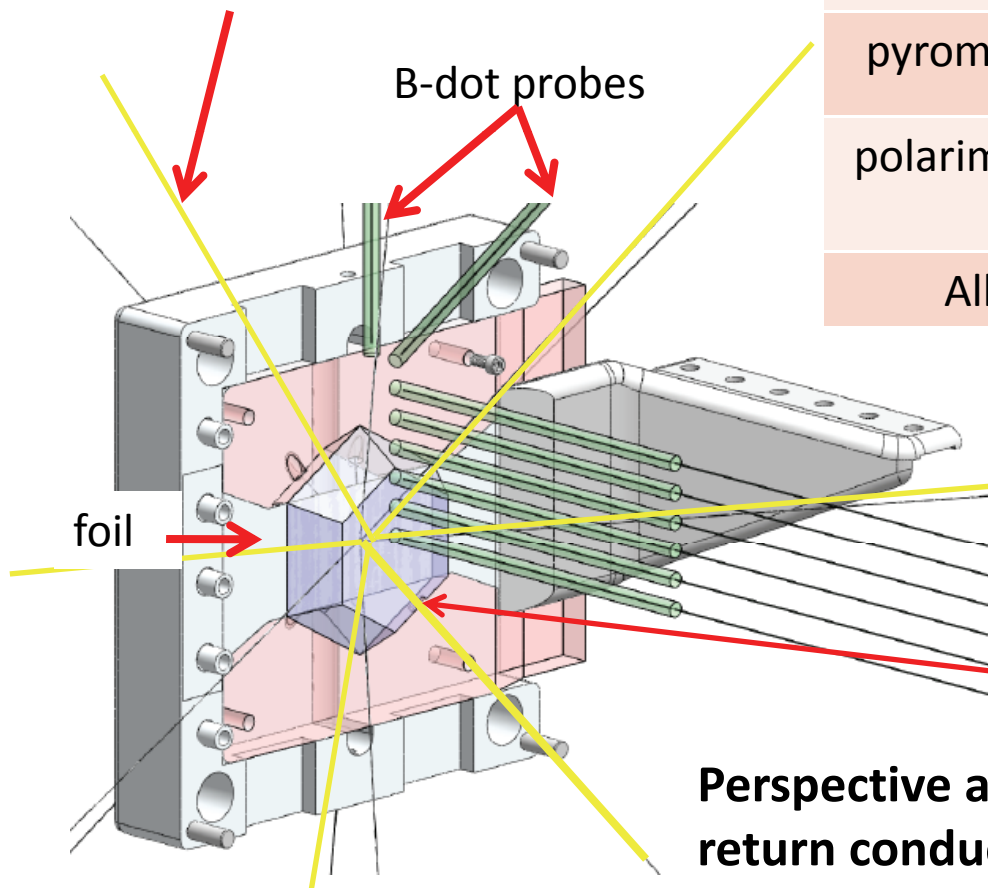


Technical Approach



Numerous lines of sight
orthogonal to tamper
facets (both sides)

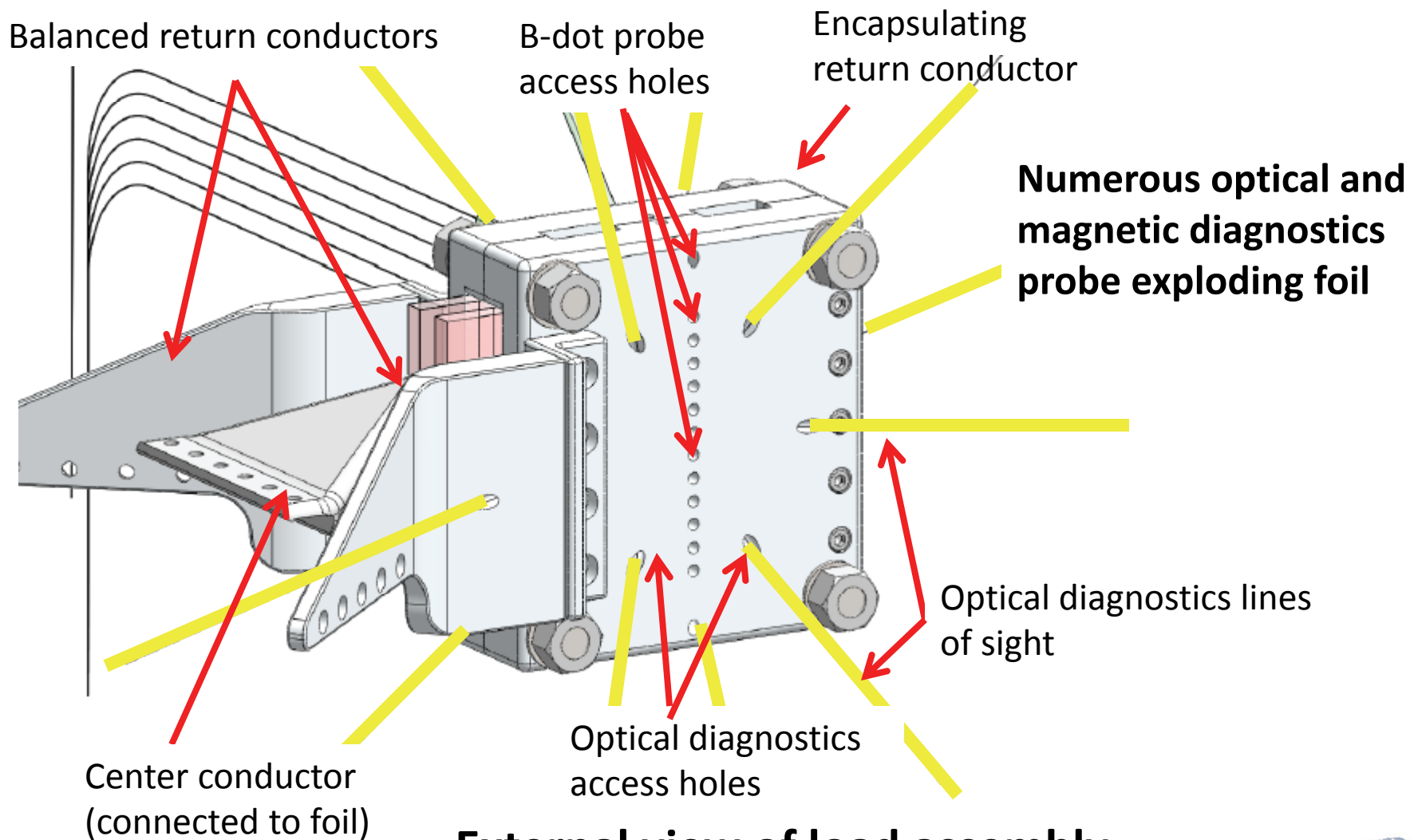
Diagnostic	Measurement	Property
B-dots	magnetic field	J
PDV	displacement	ρ , P
pyrometer	spectral radiance	T
polarimeter	s & p Amp & phase	σ , ϵ
All	All	U



**Perspective and end-on views of load with stainless steel
return conductor partially removed**



Technical Approach



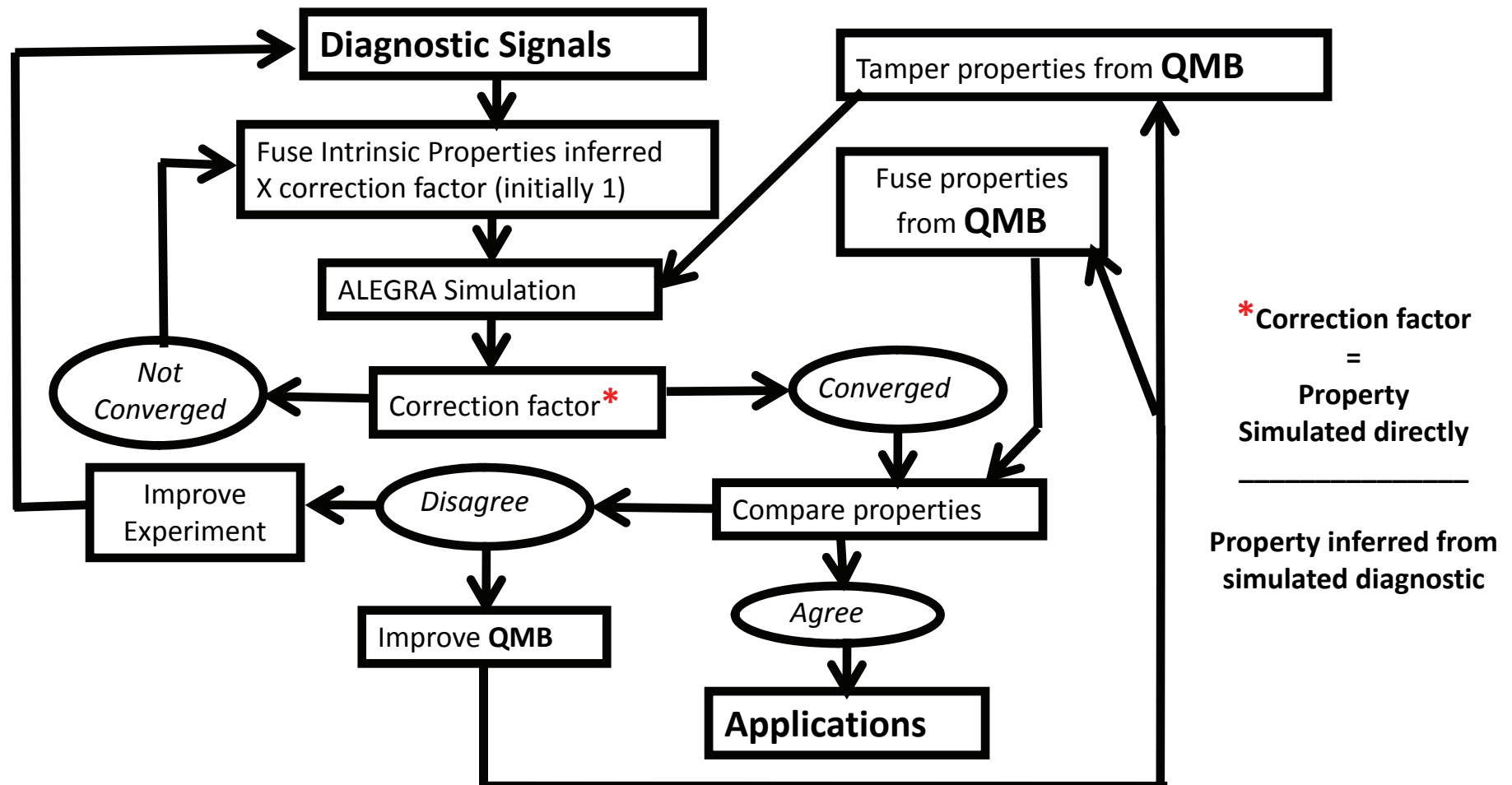
External view of load assembly

DISTRIBUTION STATEMENT A – Unclassified, Unlimited Distribution





Technical Approach



Idealized interaction of Alegra and (proposed) QMB simulations and experiment

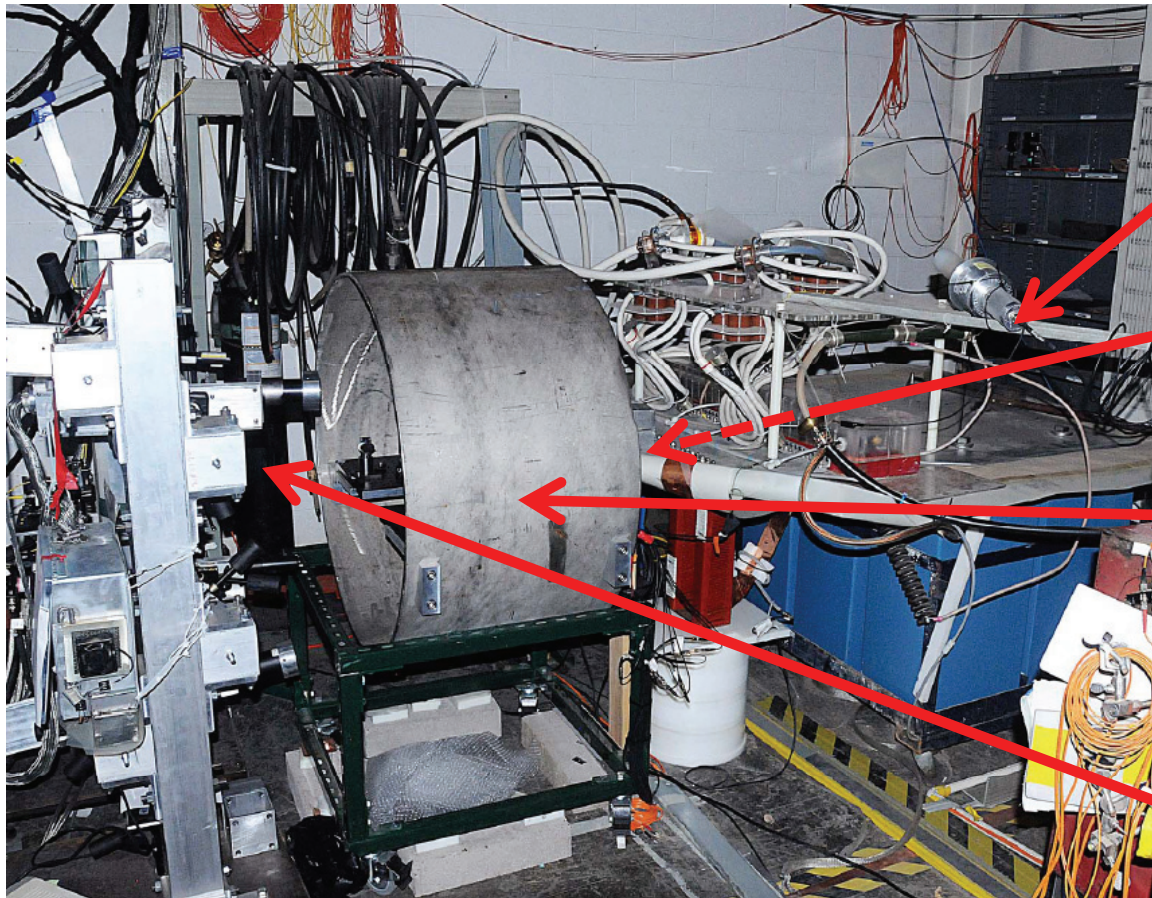
DISTRIBUTION STATEMENT A – Unclassified, Unlimited Distribution





Machine Configured for Shot 3

(Oct 22, 2012)



30 kJ capacitor bank
with reduced-noise
trigger circuit[1]

Load (inside)

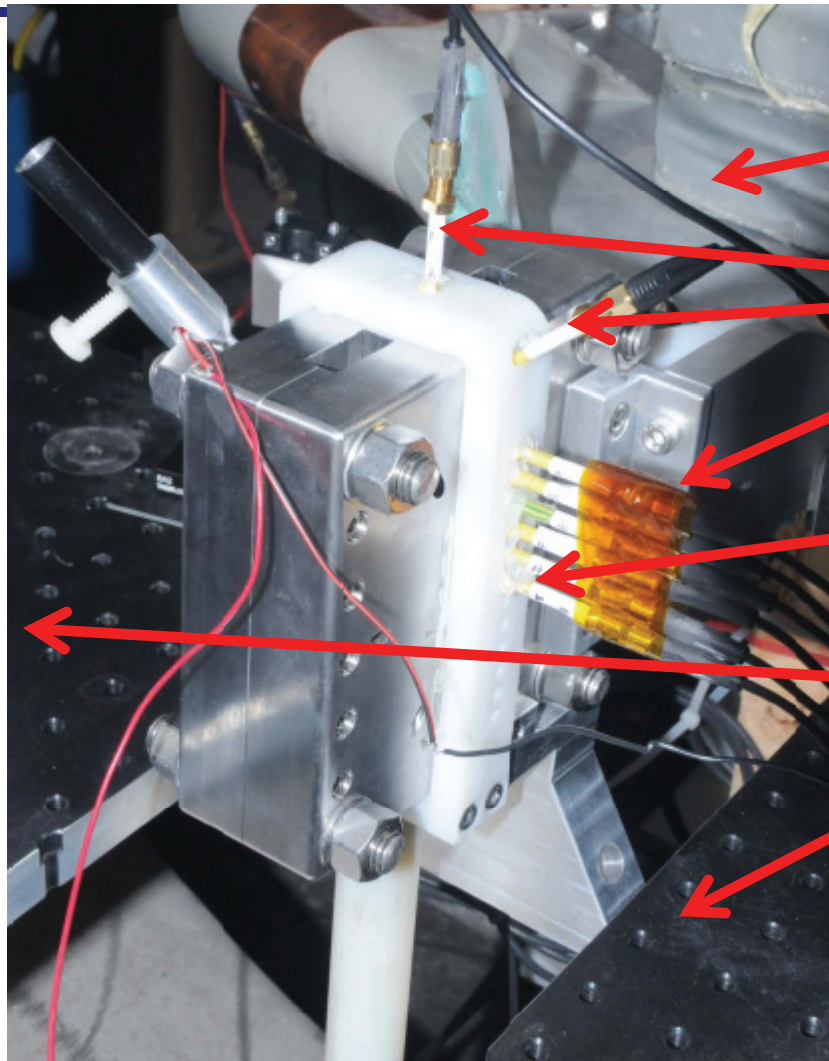
Steering mirror
breadboards in blast
chamber

Optical Diagnostic cluster

[1] E. L. Ruden, et al, Damping resonant current in a spark-gap trigger circuit to reduce noise in Proc. IEEE IPPC 2009



Load Instrumented for Shot 3



Current feed

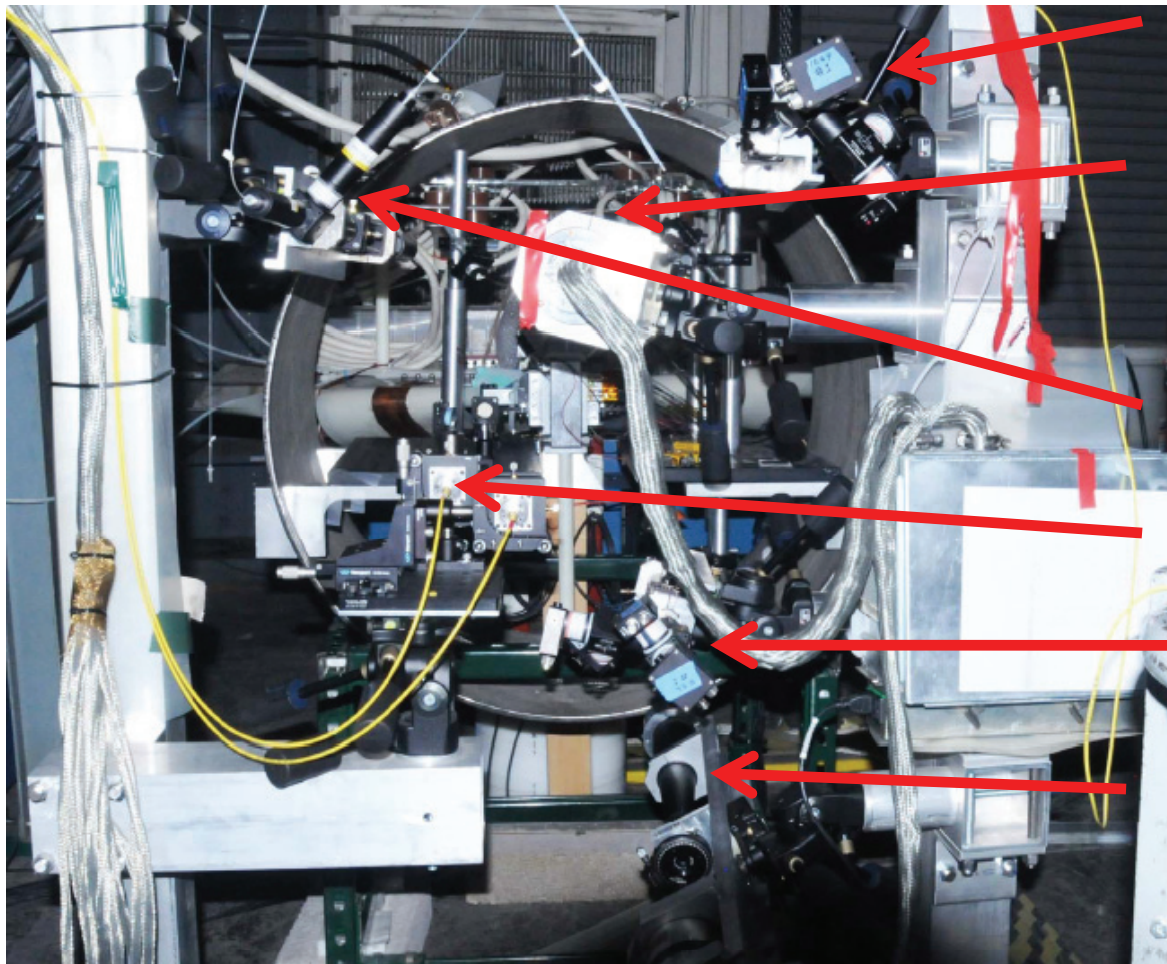
B-dot probe array (to infer surface current)

Load (S.S. return conductor visible)

Breadboards in blast chamber for optical diagnostic steering mirrors



Diagnostic Cluster for Shot 3



532nm DOAP RCVR

1064nm DOAP XMTR

Pyrometer

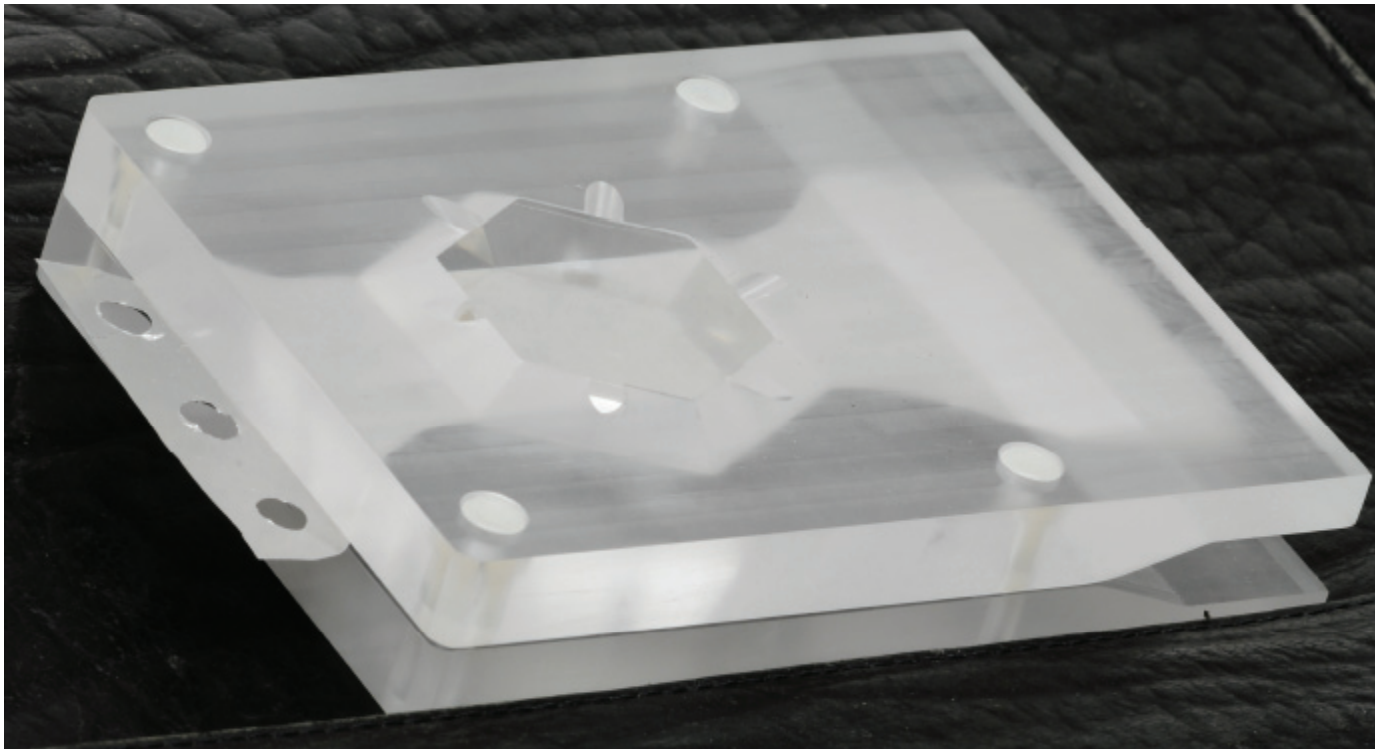
PDV XMTR/RCVR

532nm DOAP RCVR

1064nm DOAP XMTR



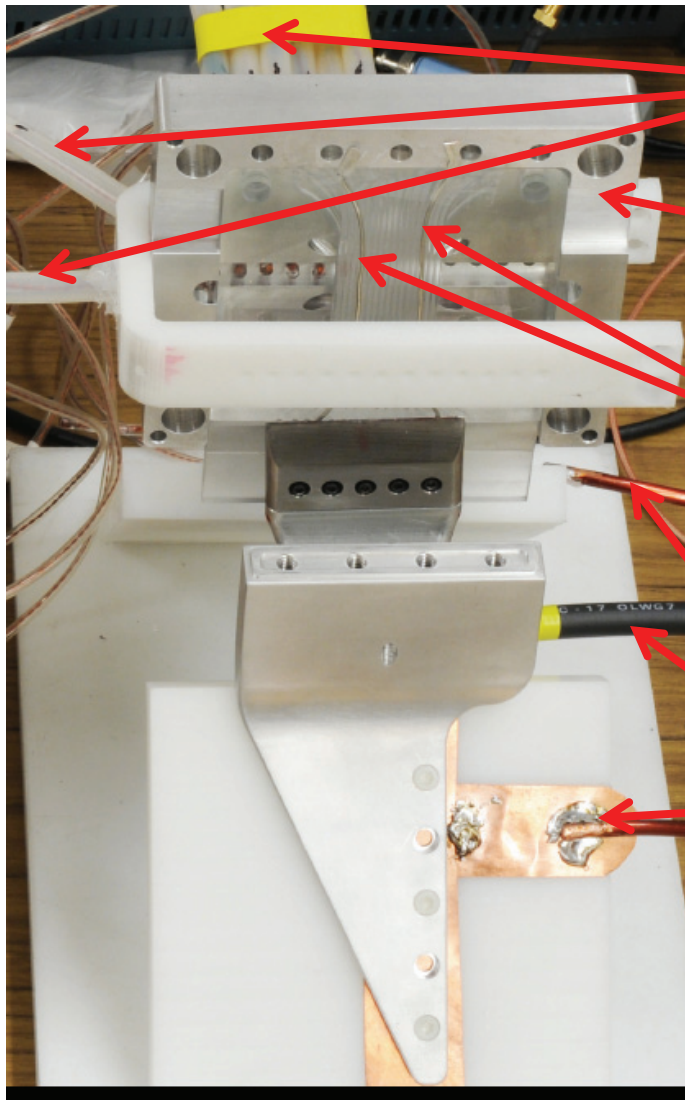
Load Foil and Tamper



For Shot 3, the hexagonal faceted tamper inserts are fused quartz.



B-dot Probe Calibration



B-dot probes (indexed $i = 1 \dots 8$ from inside-out)

Return current shell
(front half removed to show wire pair channel in special insert)

Wire pair 4 installed (indexed $j = 1 \dots 8$ from outside-in). The wire shape is determined from COMSOL simulation and is insensitive to current waveform.

Current leads to low energy pulser

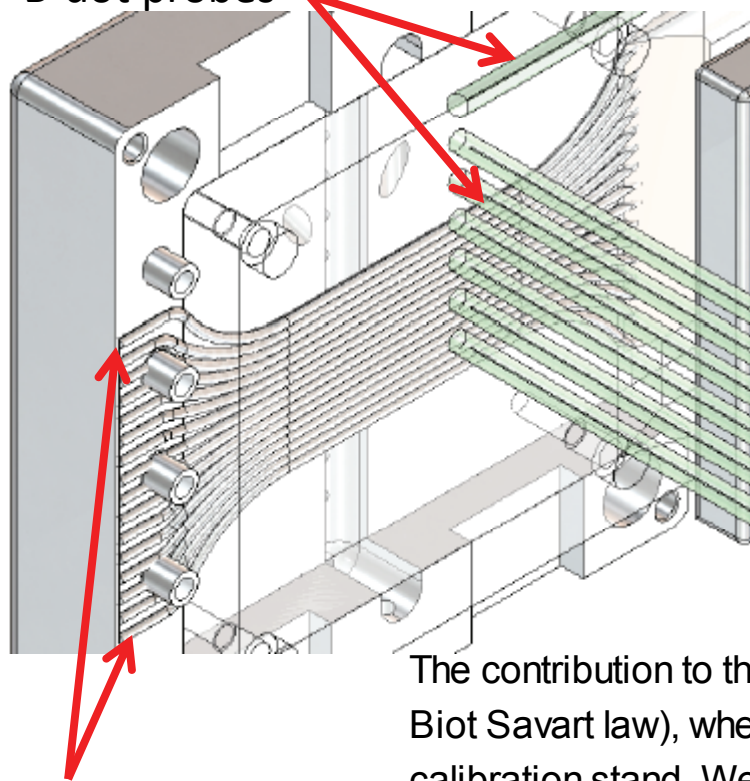
Test stand to determine calibration matrix of B-dot probe array by replacing foil with wire (element) pairs



B-dot Probe Calibration



B-dot probes



Wire pair channels
(half of return
conductor removed)

A B-dot probe array at the load midplane, covering one quadrant, is used to infer the current per unit width of foil at the midplane $\sigma(x)$ by data inversion.

For this, the foil is replaced with a series of wire pairs to represent current elements. We assume that $\sigma(x_j) = I_j/2\Delta x$ where I_j is the current in wire pair j which passes through the midplane at $x = \pm x_j$ and that Δx is the midplane wire separation.

The contribution to the time-integrated signal B_i of probe i to wire pair j is $M_{ij}I_j$ (from Biot Savart law), where (matrix elements) M_{ij} are determined empirically on the calibration stand. We then have

$$\mathbf{B} = \mathbf{M}\mathbf{I} \quad \mathbf{I} = \mathbf{M}^{-1}\mathbf{B}$$

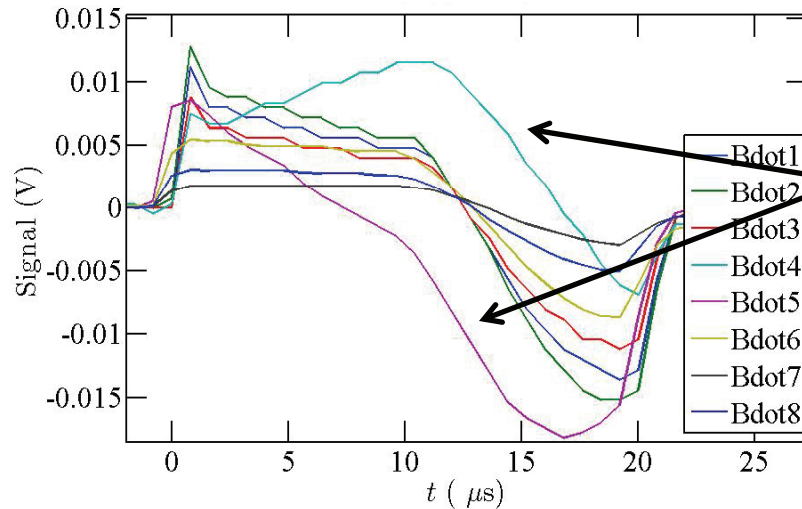
\mathbf{I} and \mathbf{B} are column vectors of the results and measurements, respectively. The second equation, then, permits estimation of σ from \mathbf{I} given fuse test measurements \mathbf{B} .



Test 3 B-dot Calibration Data

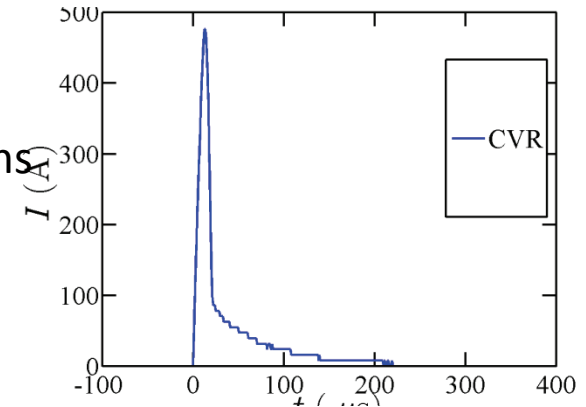


Wire pair 1 calibration B-dot signals

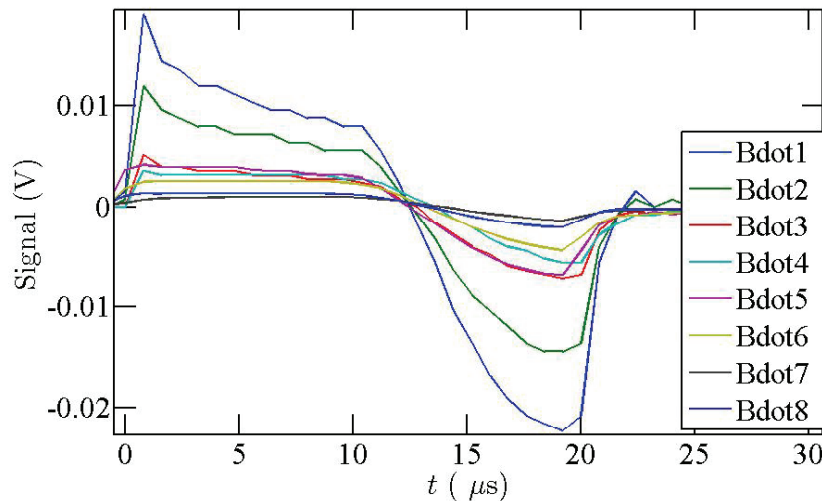


Ground loop ruins calibration

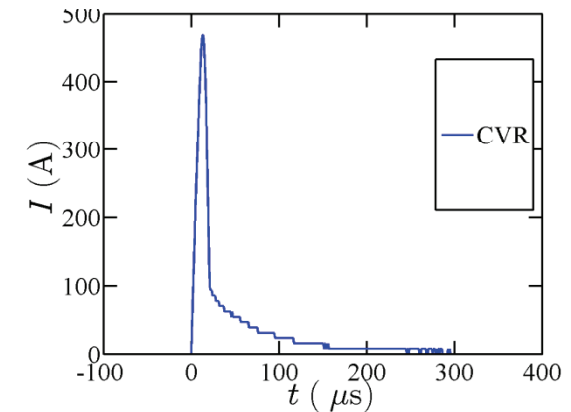
Wire pair 1 calibration current



Wire pair 8 calibration B-dot signals



Wire pair 8 calibration current



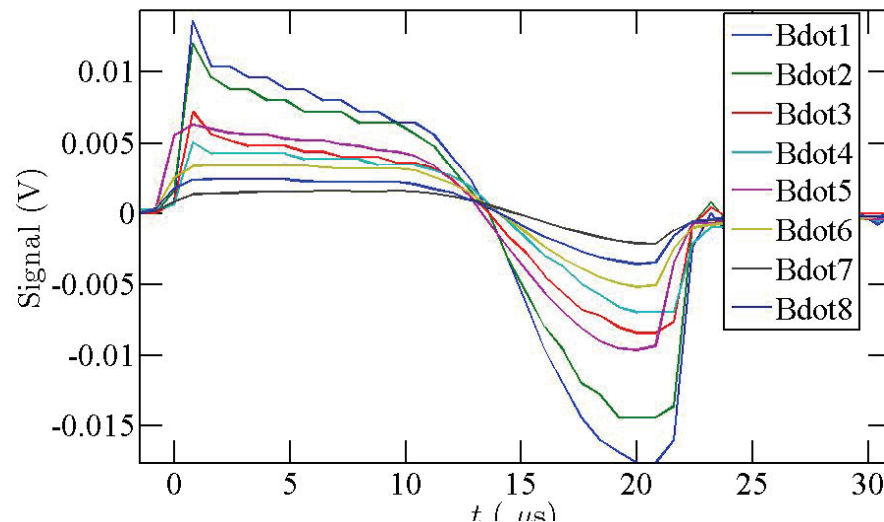
Unintegrated (raw) B-dot probe signals and wire pair currents for inner (1) and outer (8) wire pairs.



Test 3 B-dot Fuse Bench Test Analysis

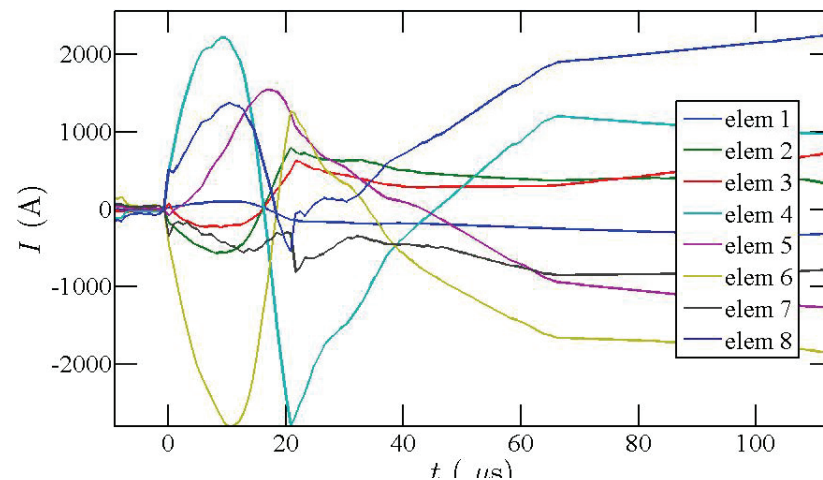


Calibration stand foil test B-dot signals (unintegrated)



To test Calibration matrix inversion method to infer the surface current density distribution, an actual fuse was placed in the load and driven by the calibration pulser. B-dots were recorded.

Inferred current elements from inverse calibration matrix multiplication method



This simple matrix inversion method is prone to numerical artifacts, such as negative-going currents. Regularization methods will be needed and the ground loop issue fixed.



B-dot Probe Analysis (Pending)



Regularized Least Squares Fit Solution to \mathbf{I}

From the principle of superposition, the set of time integrals of the p (baseline-corrected) and time integrated B-dot signals (V·s), represented column vector \mathbf{B} is,

$$\mathbf{B} = \mathbf{M}\mathbf{I}, \quad \mathbf{I} \in \mathbb{R}^q$$
$$\mathbf{M} \in \mathbb{R}^{p \times q}, \quad \mathbf{B} \in \mathbb{R}^p$$

where \mathbf{M} (V·s/A) is the B-dot probe calibration matrix, and \mathbf{I} (A) is the column vector of the q current elements quantifying the surface current. That is, M_{ik} is the sensitivity of integrated B-dot signal i to the current flowing in the discontinuous element corresponding to the path and spacing of wire pair j , as determined by bench calibration using actual wire pairs. There is, in general, a unique solution to \mathbf{I} only for $p = q$. The problem is generally underspecified or overspecified if $p < q$ or $p > q$, respectively. Even for $p = q$, though, the exact solution is found to be dominated by numerical artifacts of high spatial frequency.

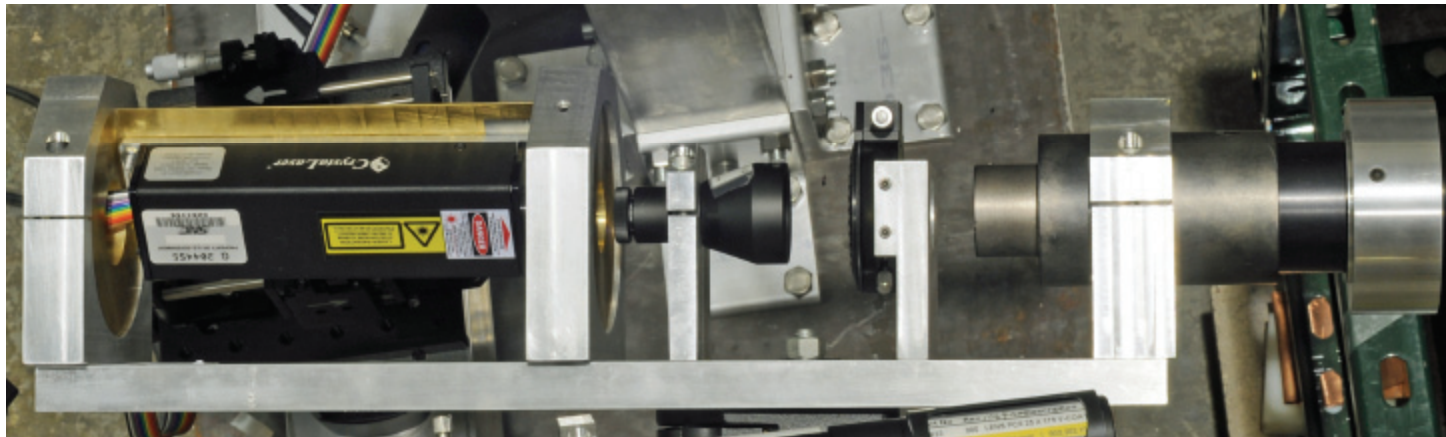
Data inversion is, instead, accomplished via linear regularizationcite: Press92. For this, an approximation to \mathbf{I} is found which minimizes,

$$|\mathbf{M}\mathbf{I} - \mathbf{B}|^2 + \lambda|\mathbf{D}\mathbf{I}|^2$$
$$\mathbf{D} \in \mathbb{R}^{r \times q}, \quad r \leq q$$

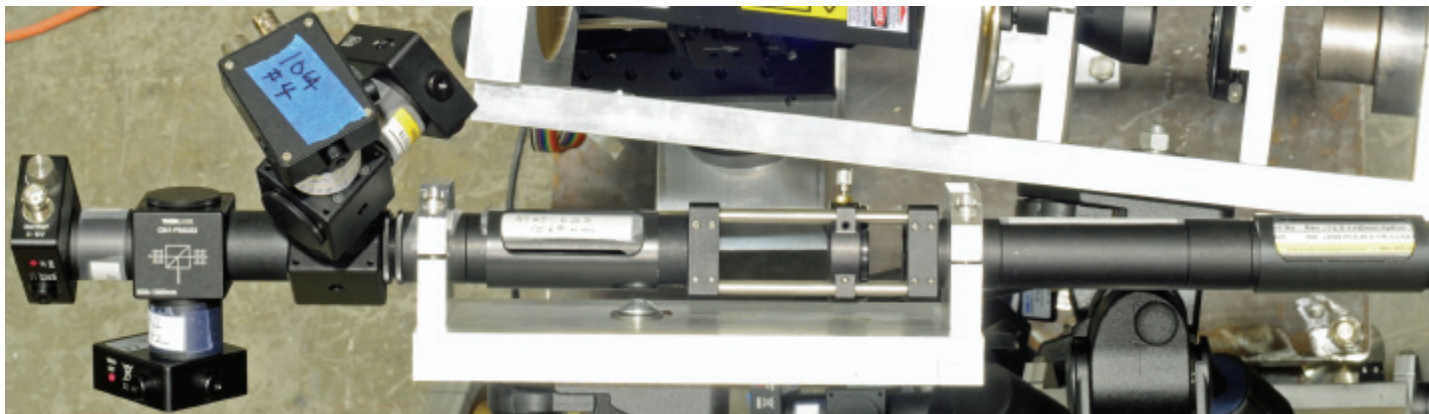
where \mathbf{D} is a matrix operator characterizing the high spatial frequencies (“noise”) we wish to suppress, λ is the weighting factor for such, $|\mathbf{X}|^2 = \mathbf{X}^T\mathbf{X}$ (scalar magnitude squared) if \mathbf{X} is a column vector (as is the case above), and superscript T means transpose.



Division of Amplitude Polarimeters (DOAP)



532 XMTR



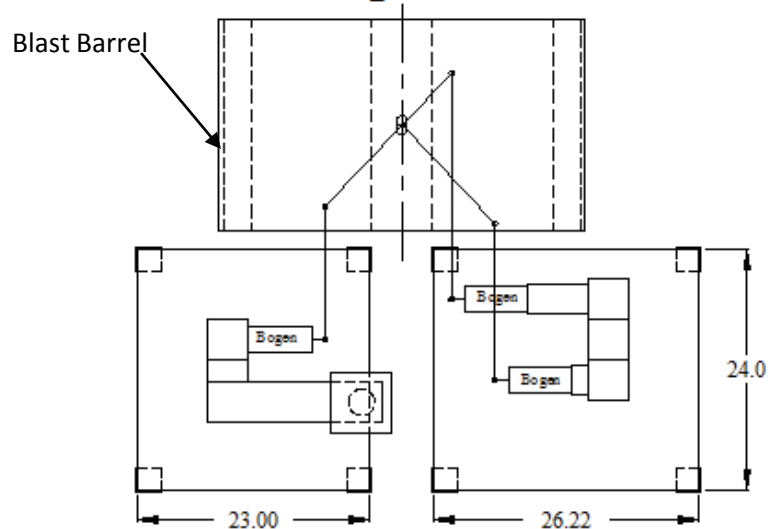
1064 RCVR



Experiment Setup

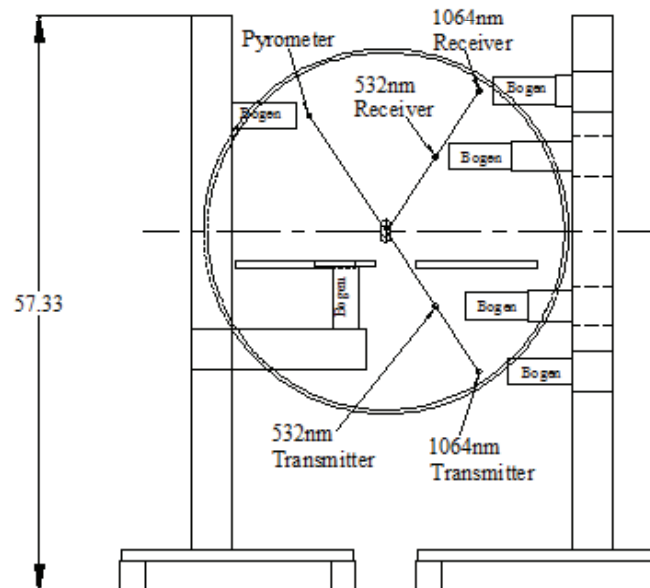


Top View

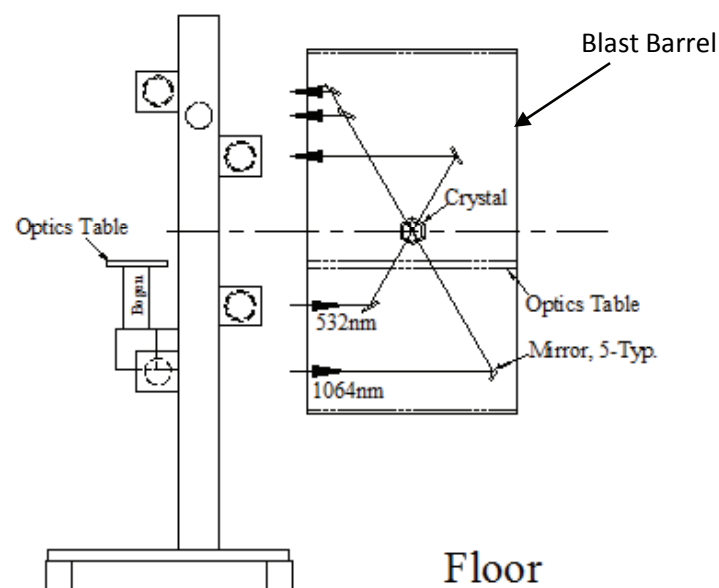


- 1064nm and 532nm laser light is transmitted from two DOAP Transmitters through the tamper and then received by the DOAP Receiver.
- Changes in polarization caused by the Load contained in the crystal are monitored by the receiver.
- The blast barrel protects expensive optics.
- A robust design allows for a vibration free optical environment.

Front View



Side View

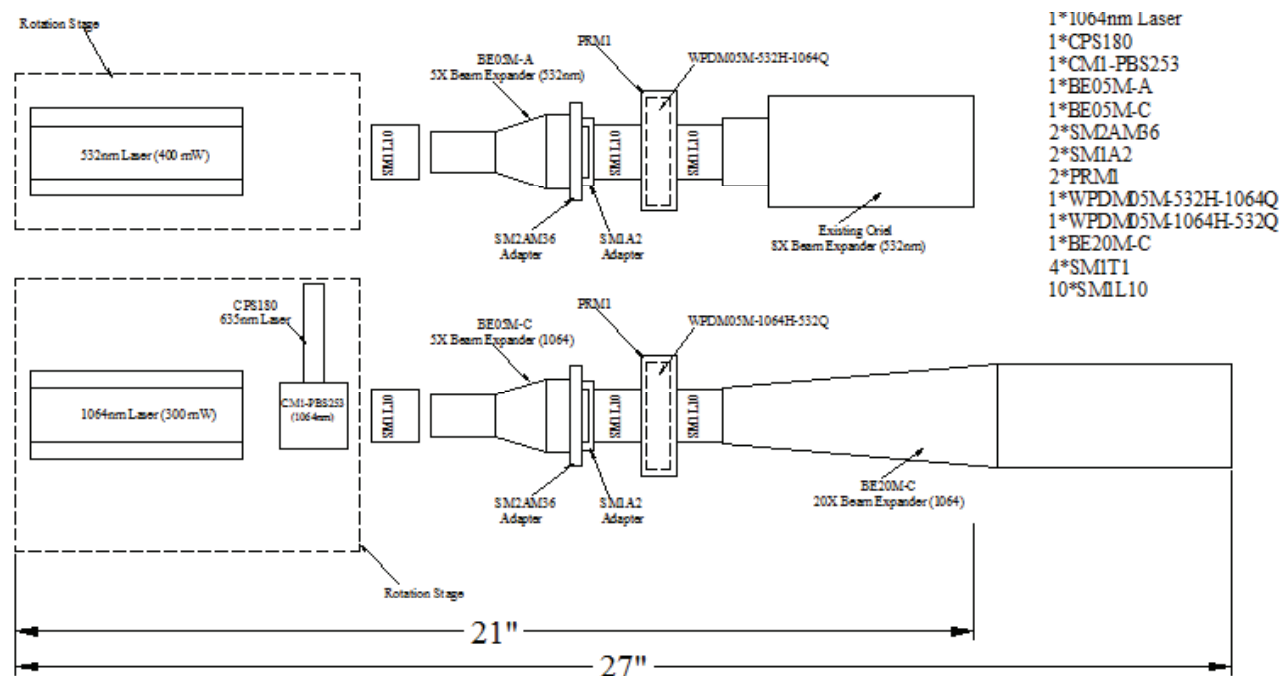




DOAP Transmitters



- The laser beam from each arm of the transmitter is expanded by a beam expander (BE05M-A, BE05M-C).
- Next the laser beam traverses a quarter wave plate (1064Q, 532Q) mounted on a rotation stage (PRM1).
- Finally the beam exits through a beam expander (Oriel, BE20M-C)
- Any polarization state can be generated by rotating the laser rotation stage and/or the quarter wave plate.

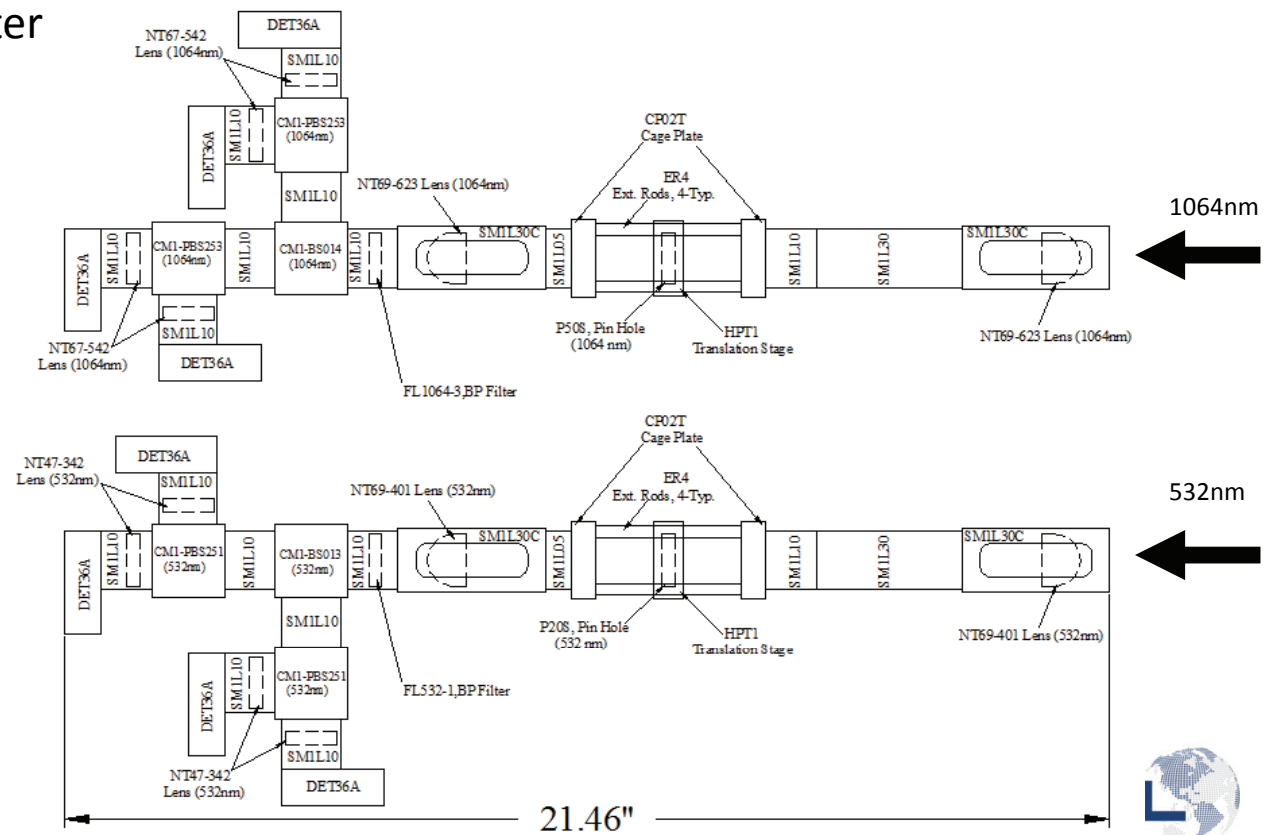




DOAP Receivers



- Light entering each receiver arm is focused onto a pinhole for spatial filtering by using a Plano-Convex (PCX) lens located at the entrance to each receiver arm (NT69-623, NT69-401).
- Light from the opposite side of the pinhole is collimated using a PCX lens (NT69-623, NT69-401).
- The light is optically filtered using a band pass filter (FL1064-3, FL532-1).
- Light is then split with a 50:50 non-polarizing beam splitter (BS014, BS013).
- The Light is split again with polarizing beam splitters (PBS251), one being rotated 45 degrees relative to the other.
- Finally the light is focused onto light detectors (DET36A) using a PCX lens (NT67-542, NT47-342).





Setting Polarization for Calibration



- The polarization of light is described the four components of the Stokes Vector
- The electrical output from the four light detectors of the receiver permit calculation of these components.
- The quarter wave plate and the polarized laser rotation stage are used to generate four known states of polarization for calibration of the instrument.
- For the actual experiment, the laser and the quarter wave plate angles were adjusted such that light incident on the load was linearly polarized at an angle of 45 degrees from the (reference) plane of incident and reflected beams (equal s and p components).

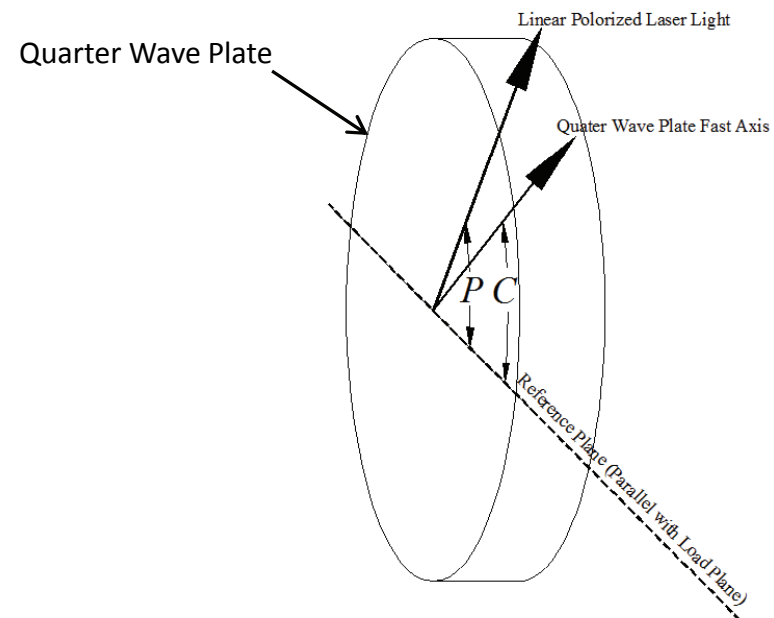
Stokes Vector

$$S_0 = 1$$

$$S_1 = \frac{1}{2} \cos(2P) + \frac{1}{2} \cos(4C - 2P)$$

$$S_2 = \frac{1}{2} \sin(2P) + \frac{1}{2} \sin(4C - 2P)$$

$$S_3 = \sin(2C - 2P)$$





Detector Response and Stokes Vector



The instrument response vector I to the Stokes vector S

$$S = [S_0, S_1, S_2, S_3]^t,$$

is given by

$$I = MS,$$

where M is a 4X4 instrument matrix and is characteristic of the instrument.

And, I is the instrument response vector and is given by four voltages (intensities)

$$I = [I_0, I_1, I_2, I_3]^t.$$

In order to calibrate the instrument, the instrument is illuminated with four linearly independent calculated states to obtain a 4X4 matrix (S_m) of Stokes vectors, corresponding to a 4X4 matrix of voltages (I_m). The columns of the Stokes matrix (S_m) are the calculated Stokes vectors of each state. The response voltages are also arranged by columns in the matrix (I_m). The response of the instrument to the calculated input states is given by

$$I_m = MS_m.$$

Where, (I_m) is the 4X4 response matrix and (S_m) is the calculated input Stokes matrix.



DOAP Calibration

The instrument matrix can be found by solving the previous equation for \mathbf{M}

$$\mathbf{M} = \mathbf{I}_m \mathbf{S}_m^{-1}$$

The four independent states are calculated using the following azimuth pairs for (P,C): (0,45),(10,0),(-50,-60), and (70,60). The resulting \mathbf{M} , for the 532nm arm of the instrument is given by

$$\mathbf{M} = \begin{bmatrix} 77.016 & 53.494 & 15.237 & -10.032 \\ 64.357 & -50.940 & -13.517 & 1.6865 \\ 74.579 & -64.775 & 9.8304 & 46.842 \\ 75.635 & 55.055 & -6.8813 & -50.469 \end{bmatrix},$$

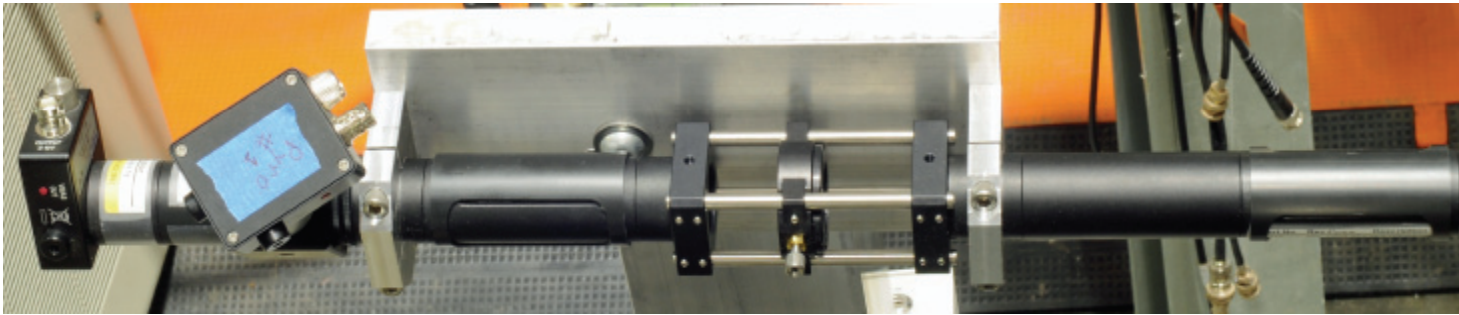
and, the resulting \mathbf{M} , for the 1064nm arm of the instrument is given by

$$\mathbf{M} = \begin{bmatrix} 34.172 & 10.372 & -2.9737 & 117.66 \\ 45.224 & 67.669 & -13.984 & 4.7525 \\ 34.008 & -3.4126 & -4.8292 & 163.98 \\ 41.114 & 80.674 & -9.3512 & -47.229 \end{bmatrix}.$$

Once the instrument is calibrated (\mathbf{M} is found), the time-dependent Stokes vector of the beam reflected from the target during the shot is $\mathbf{S} = \mathbf{M}^{-1} \mathbf{I}$, where \mathbf{I} is the detectors' response. From this we can infer the surface emissivity for the pyrometer analysis, and electrical conductivity. The latter may be extrapolated to low frequency via the Drude model for pulsed power applications.



Pyrometer



The radiant emission spectrum of a surface of wavelength-dependent emissivity $\epsilon(\lambda)$ is,

$$I(\lambda) = \epsilon(\lambda) \frac{2hc^2}{\lambda^5} \left(\exp\left(\frac{hc}{\lambda kT}\right) - 1 \right)^{-1}$$

Our pyrometer measures spectral radiance of the fuse at the two wavelengths $\lambda = \lambda_0$ and $\lambda = 2\lambda_0$, ($\lambda_0 = 532$ nm) of the DOAP's. These wavelengths were chosen so that background light for the DOAP's (for subtraction) may be determined from the pyrometry and, conversely, $\epsilon(\lambda_0)$ and $\epsilon(2\lambda_0)$ for the pyrometer interpretation may be determined by the DOAP (from the reflected Stokes vector). T may then be determined from the inverse ϵ weighted signals:

$$R \equiv \frac{\epsilon(2\lambda_0)I(\lambda_0)}{\epsilon(\lambda_0)I(2\lambda_0)} = 32 \frac{\left(\exp \frac{hc}{2\lambda_0 kT} - 1 \right)}{\left(\exp \frac{hc}{\lambda_0 kT} - 1 \right)} = 32 \left(\exp \frac{hc}{2\lambda_0 kT} + 1 \right)^{-1}$$

$$kT = \frac{hc}{2\lambda_0} \left(\ln \frac{32 - R}{R} \right)^{-1}$$

This simple formula is valid only if the longer wavelength is twice λ_0 (the shorter wavelength).

Calibration
via W
Ribbon lamp

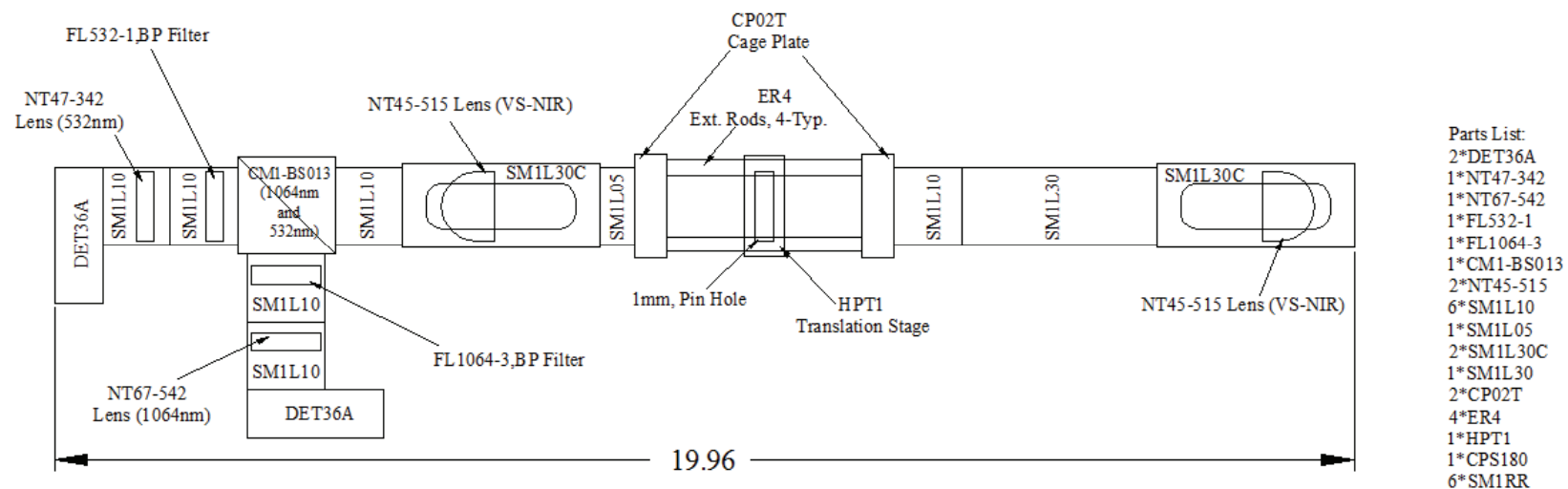




Pyrometer

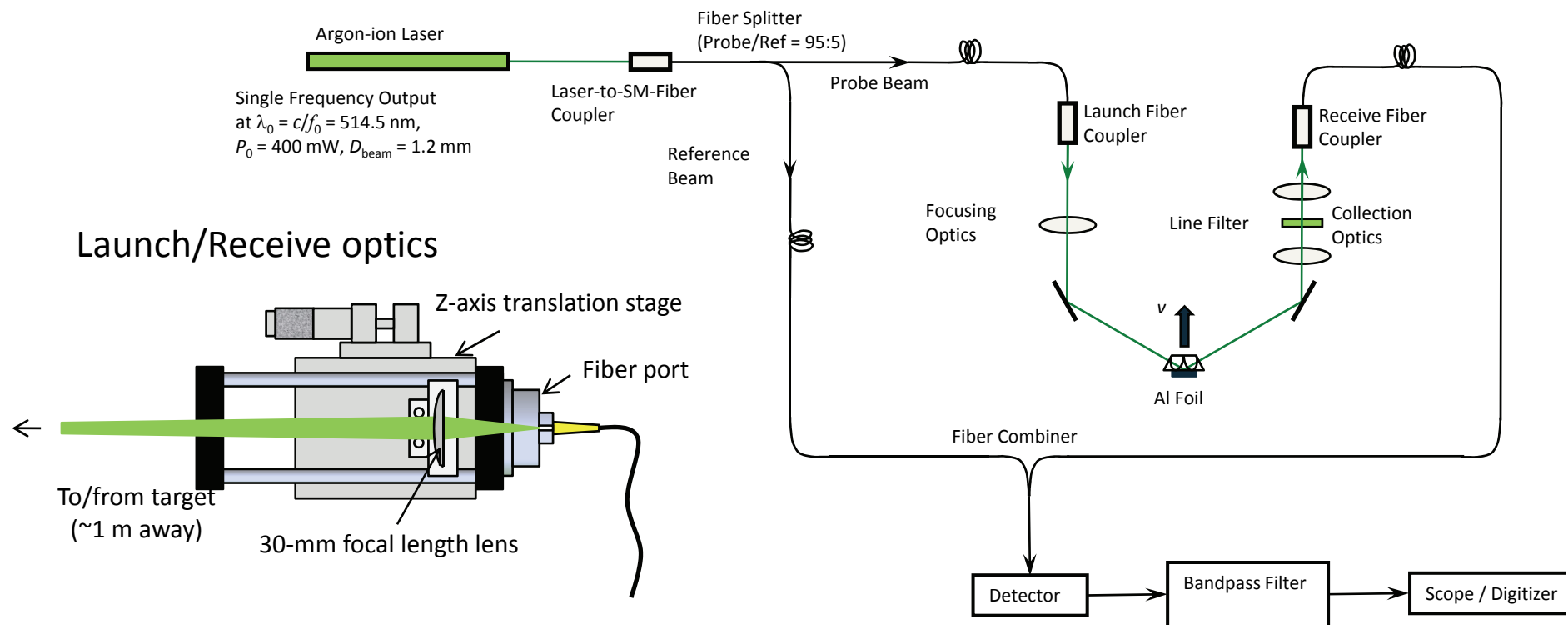


- Light entering the pyrometer is focused onto a pinhole for spatial filtering using a Plano Convex (PCX) lens located at the entrance to the pyrometer (NT45-515).
- Light from the opposite side of the pinhole is collimated using another PCX lens (NT45-515).
- Light is then split with a 50:50 polarization insensitive beam splitter (BS013).
- The light is optically filtered using a band pass filters (FL-532, FL1064) to record 532nm and 1064nm intensities, respectively.





PDV



Bandpass filter output is a beat wave signal at $f_b = |f_d - f_0|$, where $f_d = (1 + 2\beta \cos\theta)f_0$ is the Doppler-shifted frequency ($\beta = v/c$, θ = angle of incidence)
 $\rightarrow f_b = 2f_0 \beta \cos\theta$, so for $\theta = 60^\circ$,
 $f_b / v = 1.94 \text{ GHz / km / s}$.

Initial version of PDV (to measure foil expansion velocity) assembled but untested



ALEGRA Simulations

(See poster, this conference, David Amdahl, et al)



ALEGRA, a parallel, 3D RMHD code will be used to provide self-consistent data tables

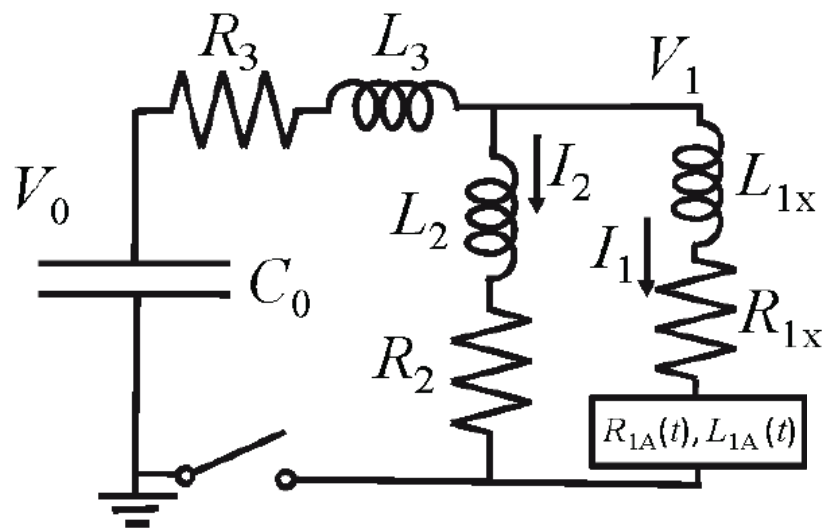
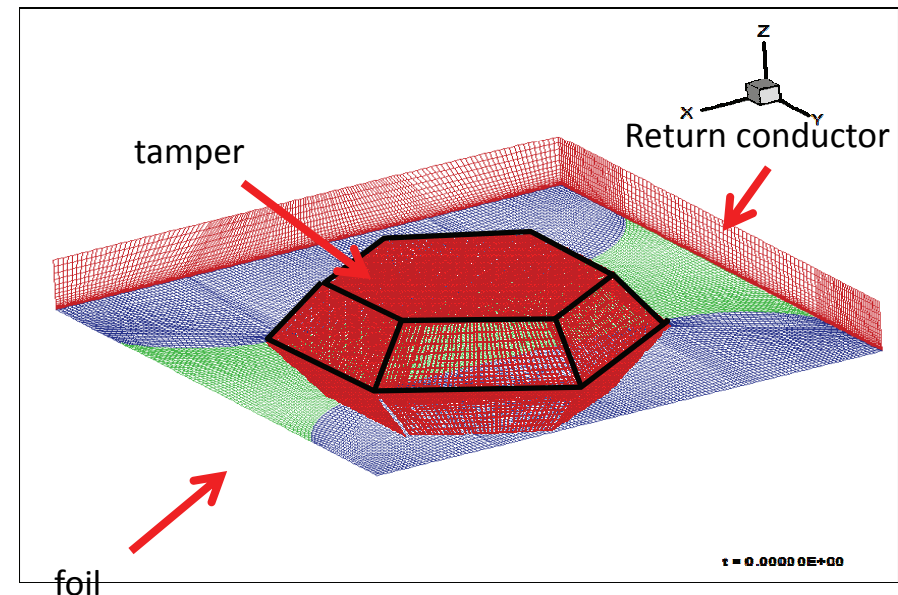


Fig. 1 Assumed Circuit. $L_1 = L_{1X} + L_{1A}$ and $R_1 = R_{1X} + R_{1A}$, being the sum of external and ALEGRA contributions. The X terms, needed for external couple circuit modeling, must be determined by subtraction of A terms, determined by ALEGRA simulation.

3-D mesh of load geometry to be run on ALEGRA





External Coupled Circuit Model



Parameter	value DEF	Units (MKS)
Bank capacitance	$C_0 = 35.44 \times 10^{-6}$	F
Effective bank charge $V_0(0)$	$0.98 \times V_{00}$ actual	V
Shunt resistance	$R_2 = 30.44 \times 10^{-9}$	Ω
Load inductance	$L_1 = 4.503479 \times 10^{-8}$	H
Shunt inductance	$L_2 = 5.190187 \times 10^{-7}$	H
Railgap inductance	$L_3 = 3.098713 \times 10^{-8}$	H
Railgap resistance	$R_3 = 3.802119 \times 10^{-3}$	Ω
Dummy load resistance	$R_1 = 12.4 \times 10^{-4}$	Ω

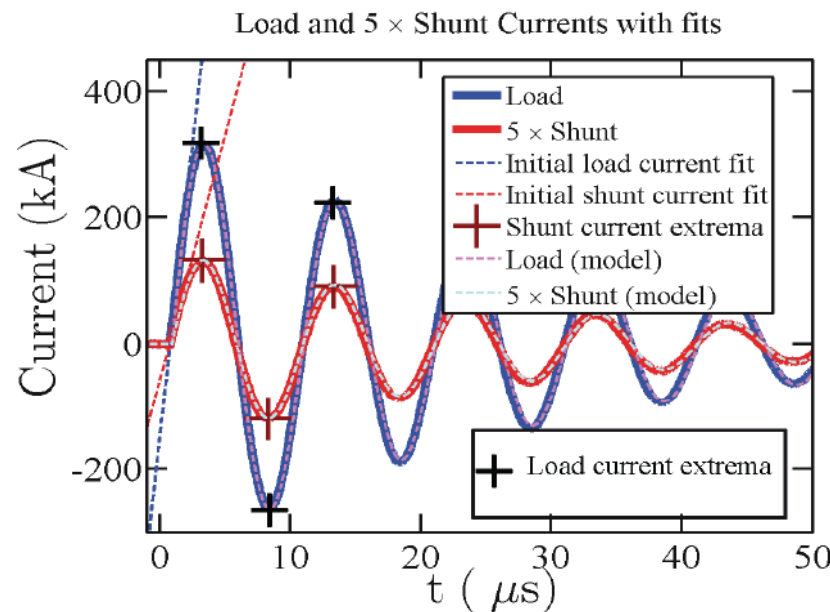


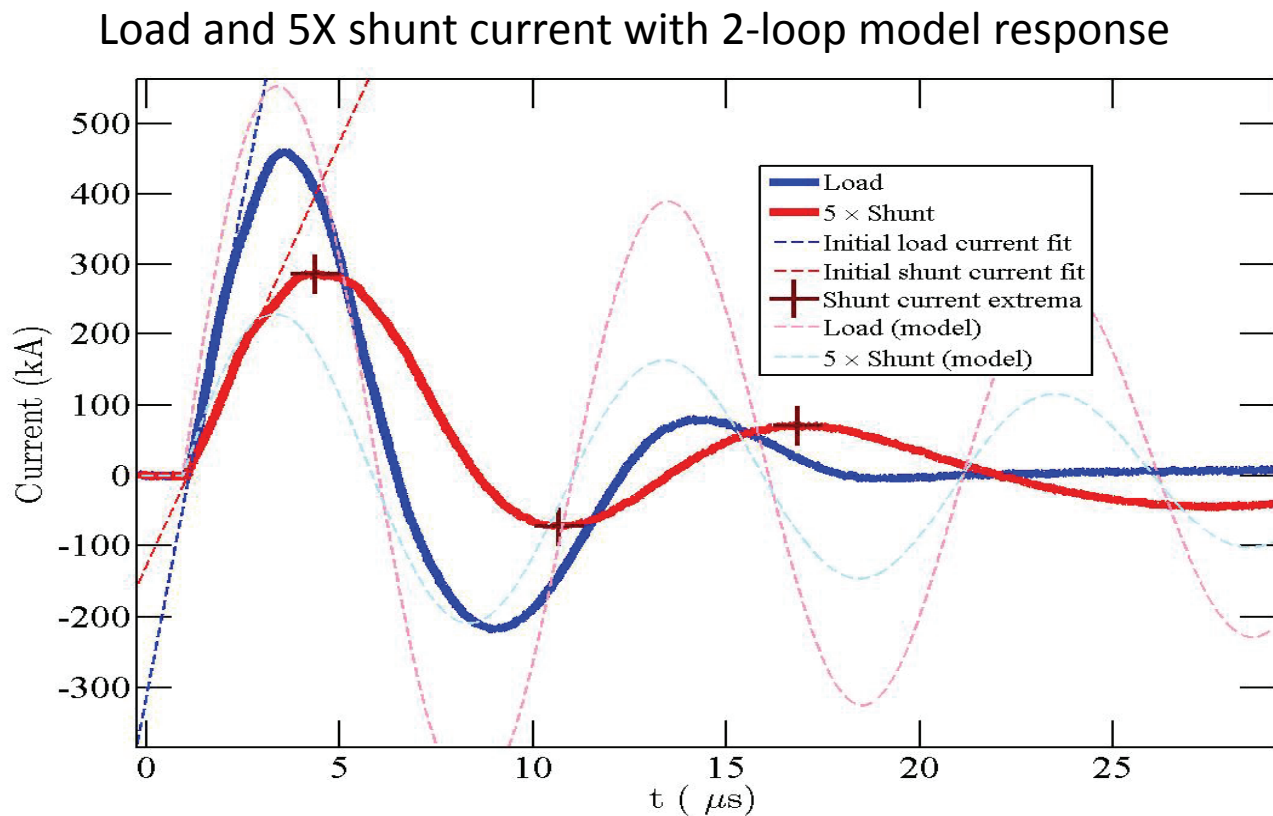
Fig. 3 I_1 (load) and I_2 (shunt) currents for shot 03-15-2012 t07. Two loop model of theoretical dummy load response overlaid, multiplied by 0.98 (17.2/21.0) since this shot had $V_{00} = 17.2$ kV actual.

Two complementary tests are used to characterize the two-loop lumped circuit model assumed to be externally coupled to the ALEGRA simulations. A high degree of precision is obtained with a dummy load test (where load remains conductive with little resistance change), as shown at here.

See other poster Ruden, et al, this conference, for details.



Shot 3 Results



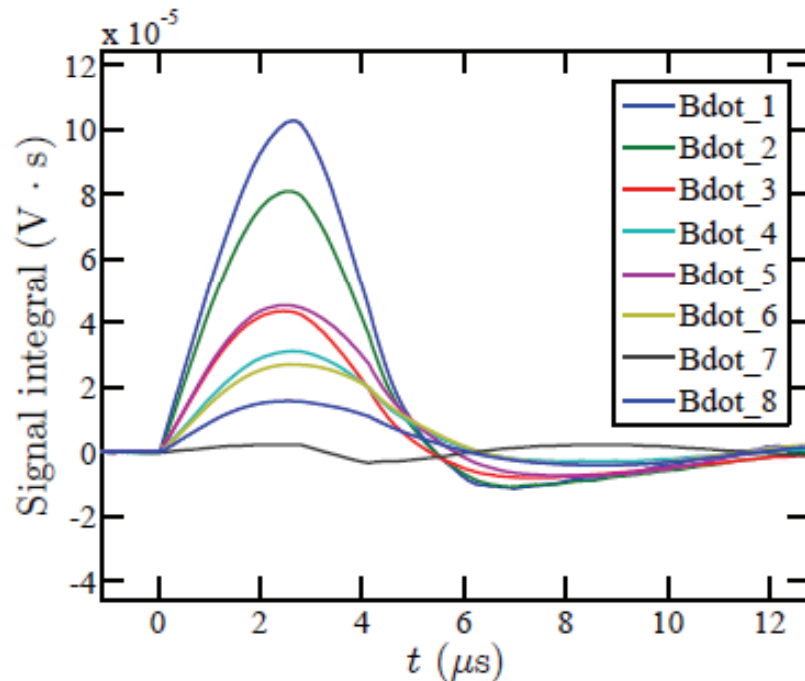
Deviation of current waveform from lumped circuit model (which assumes shunted load) is due to growing resistance of load.



Shot 3 Results

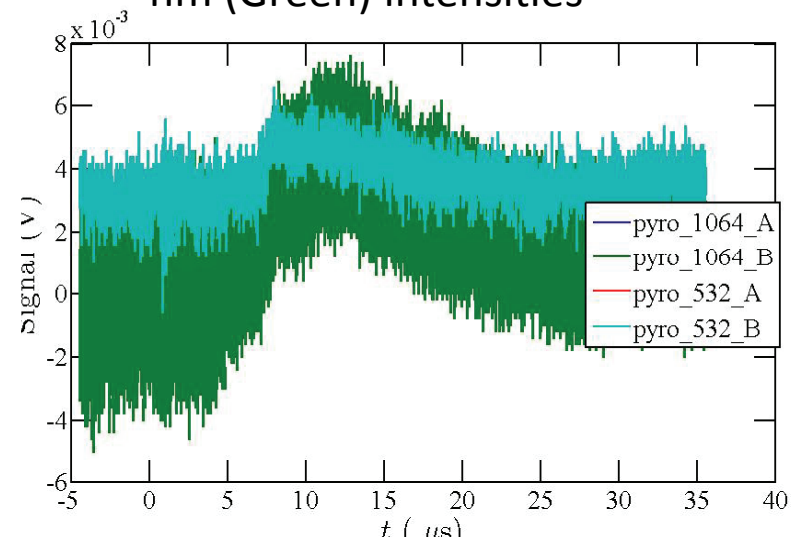


st Time integrated B-dot probe signals



B-dots look highly interpretable, except for probe 8 and given better calibration data and regularized inversion method (pending).

Pyrometer, 1064 nm (Blue), 532 nm (Green) intensities



Pyrometer is fine; we just need higher T. pending:

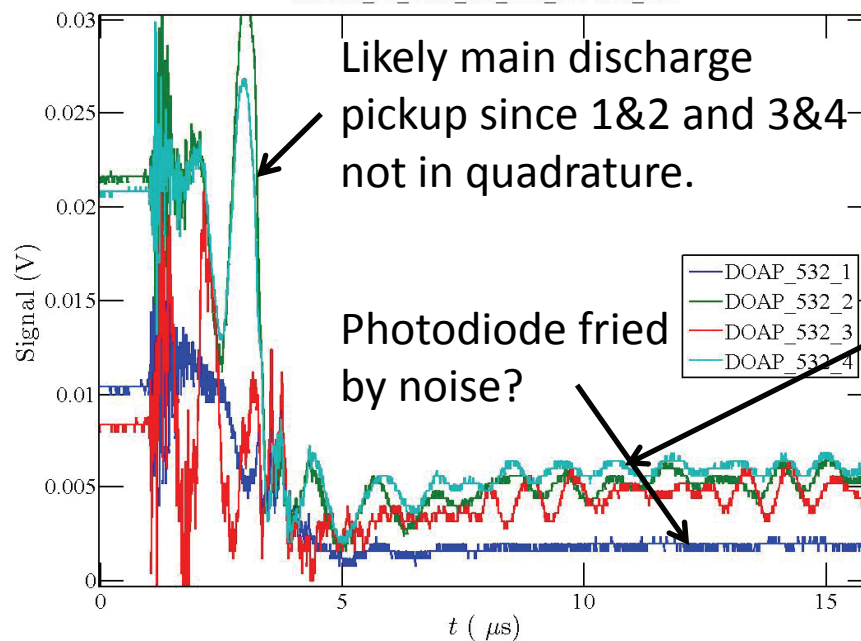
- Conversion to spectral T
- Profile foil so it gradually narrows in middle (1/2 current width).



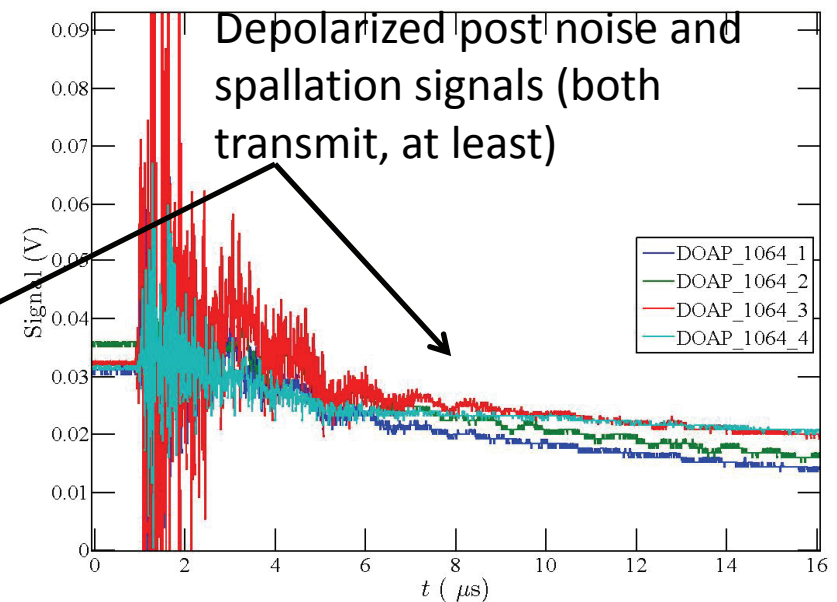
Shot 3 Results



DOAP, 532 nm laser



DOAP, 1064 nm laser



DOAP data not interpretable, but provide informative info regarding post-spallation transmission.

Pending:

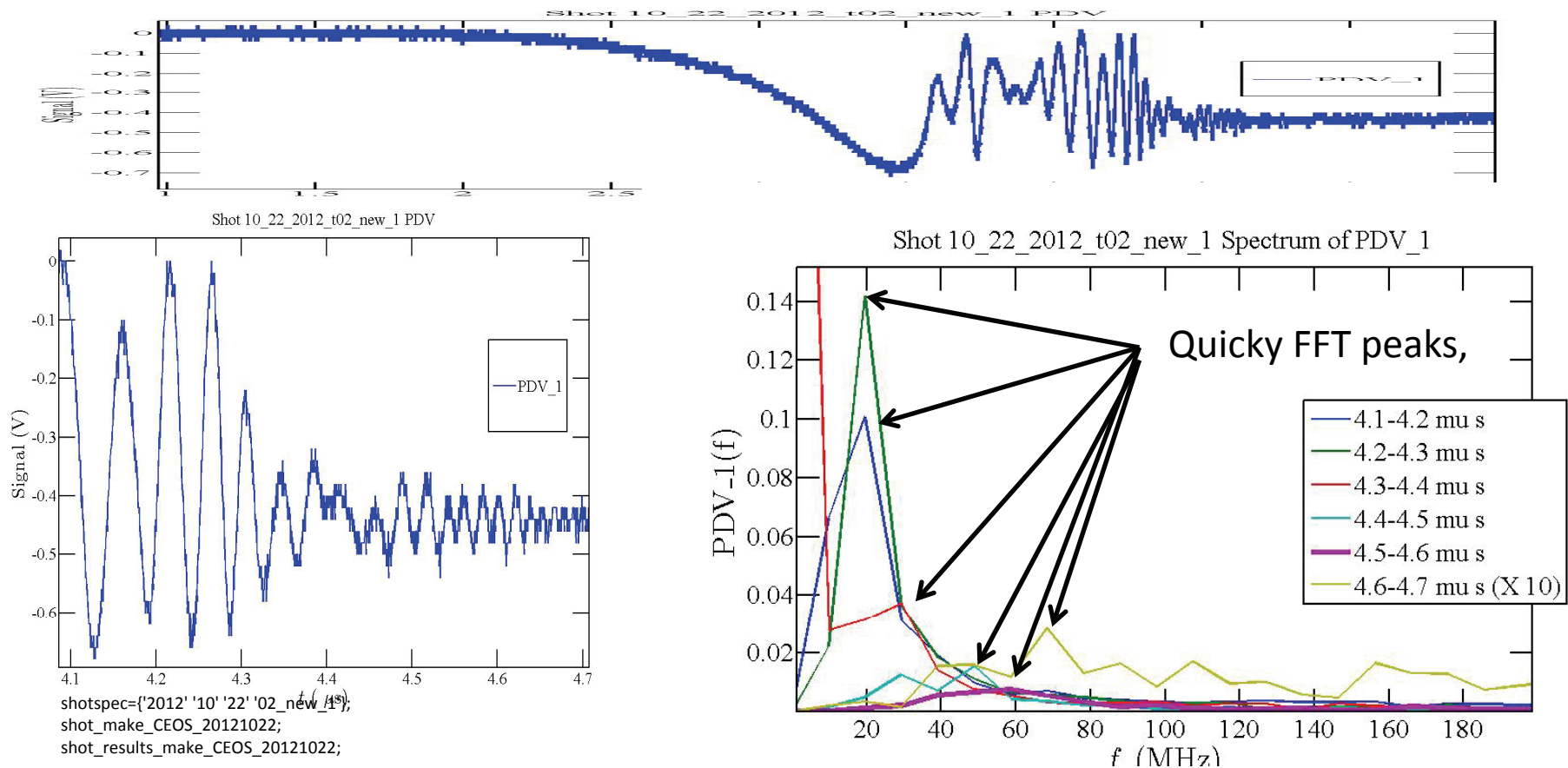
Shield Diodes and scopes in local box with fiber optic transmission of light from DOAPS



Shot 3 Results



PDV signal, closeup, and FFT of 100 ns intervals



Initial analysis suggests data interpretable via standard Hamming filter analysis and higher bandwidth record (pending). Pending: Upgrade to 2 channels and implementation of 4 GHz.



Present Status

- Diagnostic noise suppression measures implemented and tested by destructive Shot 3 (22OCT012. All passed except DOAP (need fiber optic connection to shielded optical receivers).
- Preliminary analysis of Shot 3 data suggests several diagnostic improvement should result in highly interpretable data for next shot (Scheduled for Apr 15).
- PDV being upgraded to two channels of much higher bandwidth. Both sides of fuse will be diagnosed to isolate translation component.
- Two-loop circuit parameters for main bank determined (for ALEGRA coupled-circuit) finished.
- ALEGRA simulations well developed (Dave Amdahl's poster) and producing results directly comparable to experiment (comparison pending).



Remaining Goals for FY13

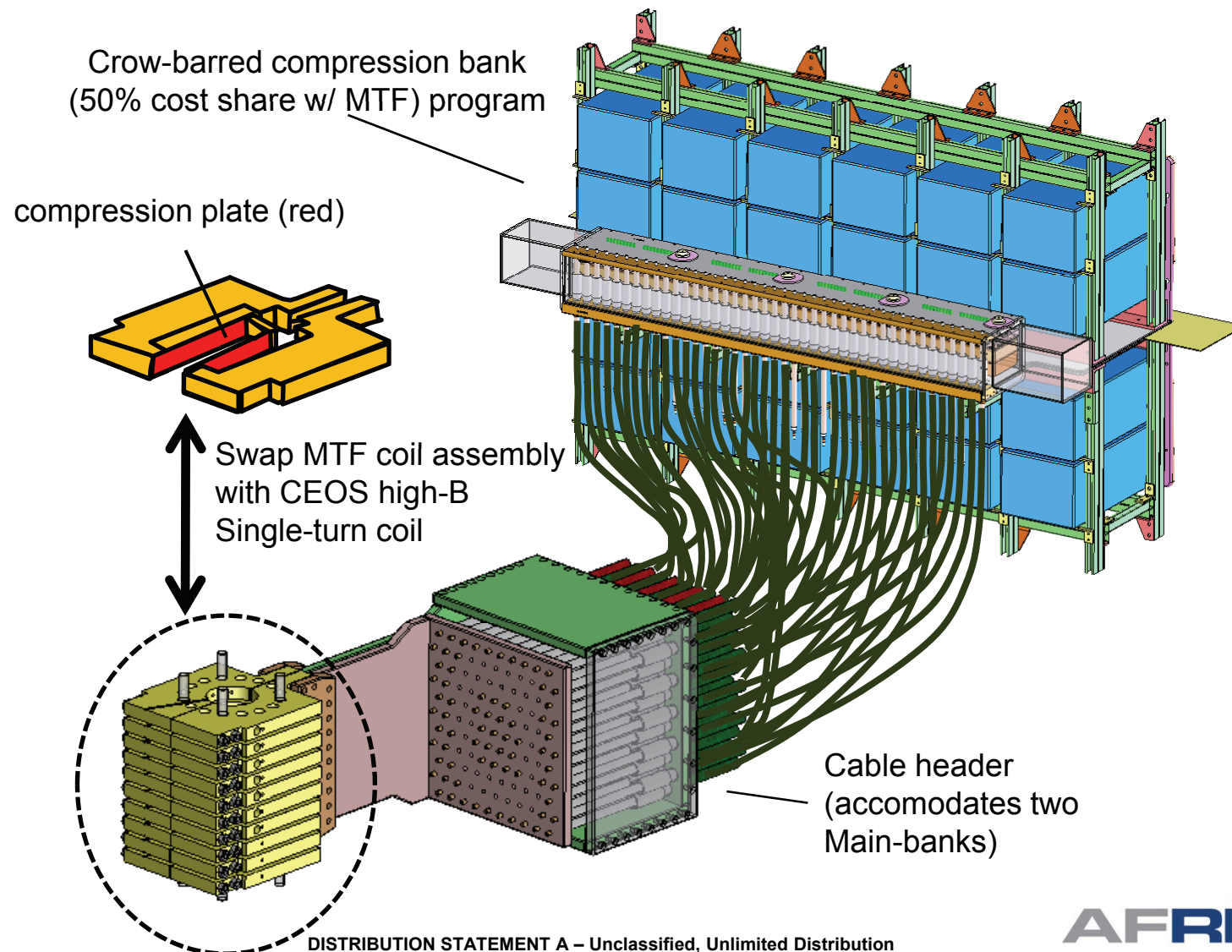


- All diagnostics and data analysis MATLAB routines calibrated and working properly.
- Properties inferred by analysis along experimental trajectories for at least one shot.
- 3-D ALEGRA simulations with external coupled two-loop circuit, fused quartz tamper, and ray-traced diagnostic simulations, and with Phase II precompression.
- Preliminary design of Phase II system based on ALEGRA simulations.



Remaining Goals for FY13

Phase II Compression Bank Design Initiation



DISTRIBUTION STATEMENT A – Unclassified, Unlimited Distribution



ALEGRA Simulations Supporting Electrical Conductivity and Equation of State Measurements of a Tampered Electrically Exploding Foil

Edward L. Ruden, David J. Amdahl, Rufus H. Cooksey, Paul R. Robinson,
and Matthew T. Domonkos

Air Force Research Laboratory, Directed Energy Directorate,
AFRL/RDHP, 3550 Aberdeen Ave SE
Kirtland AFB, NM 87117-5776 USA

Francis T. Analla, Darwin J. Brown, and Mark R. Kostora
Science Applications International Corporation
Albuquerque, NM 87106 USA

J. Frank Camacho
NumerEx, LLC
Albuquerque, NM 87106 USA

Outline

- Abstract
- ALEGRA
- Impact to C-EOS
- Comparisons of simulations of “legacy” design & new curved shape design
 - Current profiles, temperature, deformation
- Future work

Abstract

The Air Force Research Laboratory is conducting a series of experiments to improve the equation-of-state database of electrically conducting materials in the dynamic state of warm, dense matter. These experiments are supported with simulations involving resistive, magnetohydrodynamics with thermal diffusion and material strength. The three dimensional simulations are performed using ALEGRA, an arbitrary Lagrangian-Eulerian (multiphysics) computer code developed at Sandia National Laboratories¹. ALEGRA simulations supported the development of a two-loop circuit model, calculated initial experimental results, and designed a new fuse shape to enhance the experiment's performance. Experimentally, the warm, dense matter is produced by Ohmically exploding a 80 μm aluminum foil sandwiched between dielectric tampers. The pulsed power system is a 36 μF capacitor bank charged to 30.1 kV and discharged in 2.55 μs to a peak load of 460 kA. Relationships between electrical conductivity and equation of state properties such as pressure, density, temperature, specific energy, electrical conductivity, and emissivity in the ranges of up to a few eV and down to 0.1 solid density is experimentally measured.

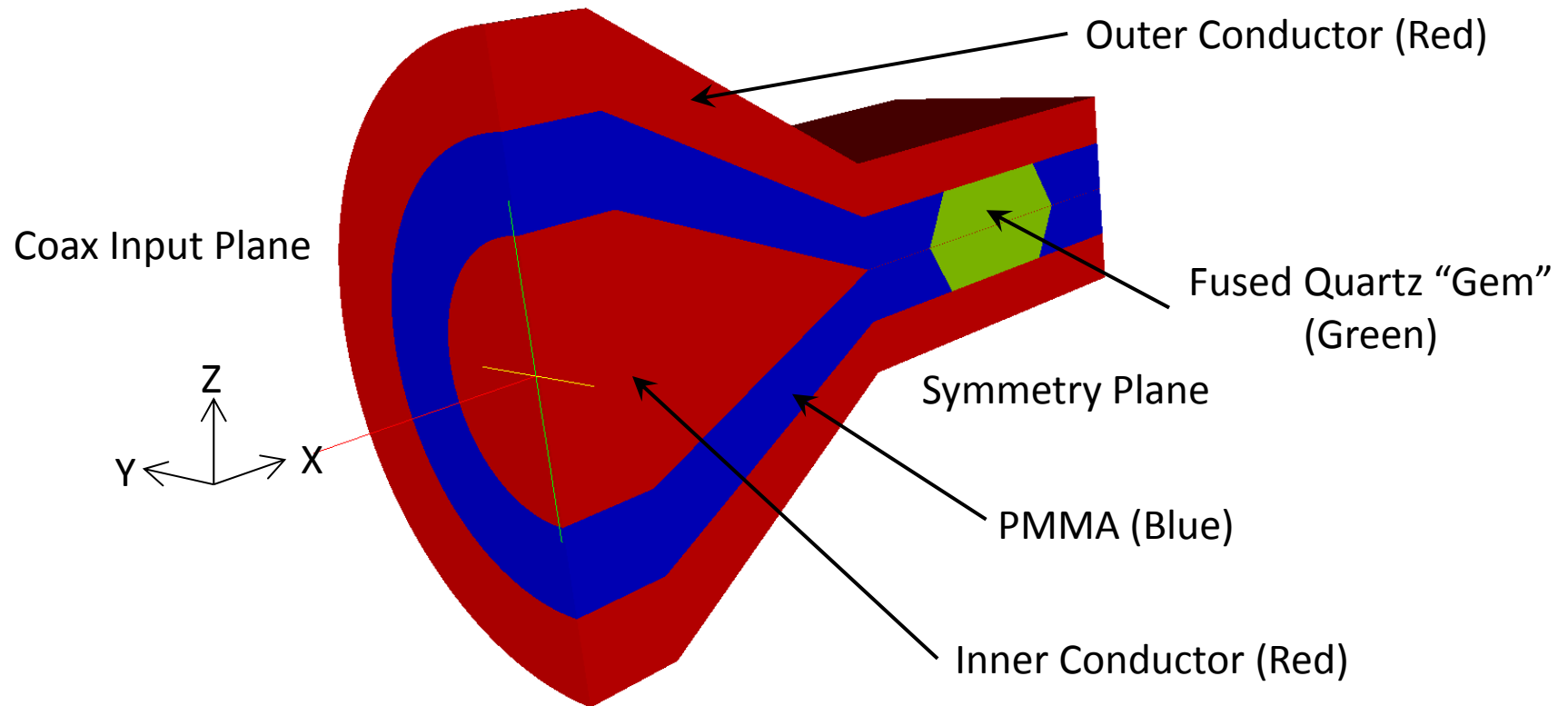
ALEGRA Simulations

- ALEGRA
 - Arbitrary lagrangian/eulerian, multiphysics computer code developed at Sandia National Laboratory
- AFRL applying ALEGRA to Conductivity and Equation of State (C-EOS) experiment
 - 3D, eulerian simulations
 - Physics: Resistive magnetohydrodynamic with thermal diffusion and material strength
 - Coupled to two-loop circuit model
 - Simulations focused on experiment's first 4 μs —just past peak current
 - Tamper constructed of fused quartz “gem” surrounded by PMMA material

ALEGRA Simulations

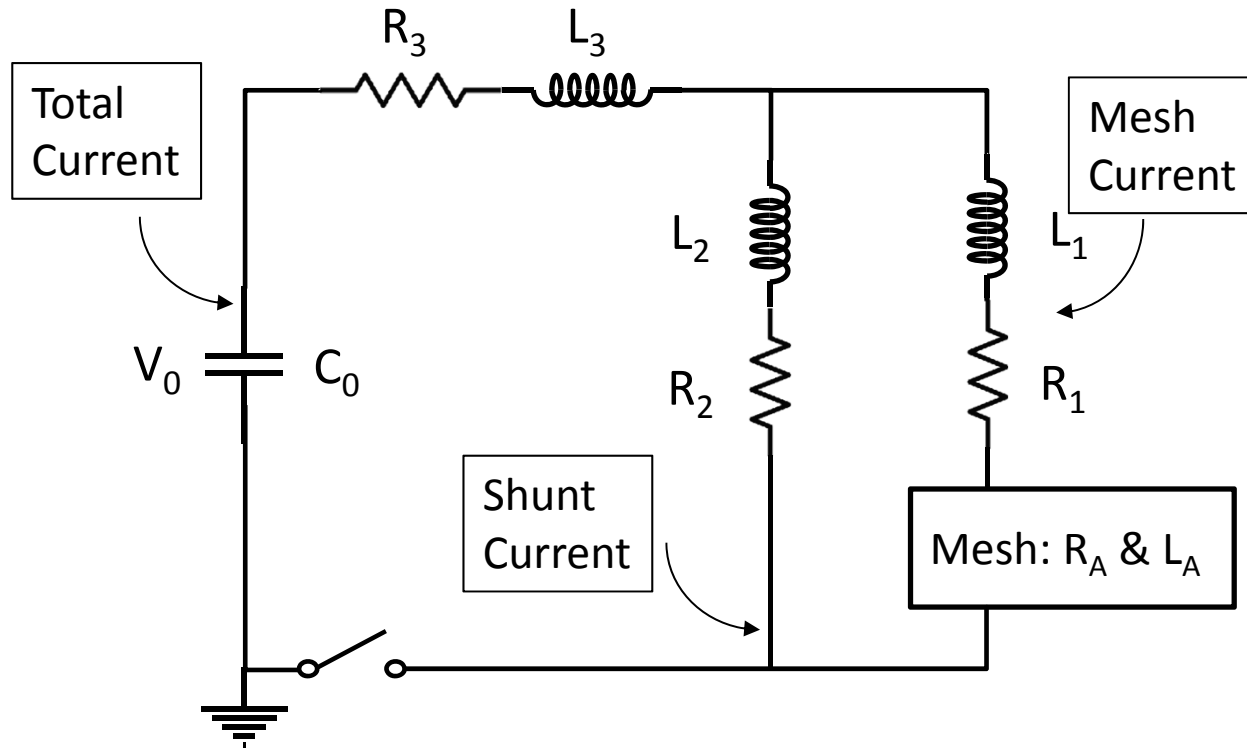
- Completed simulations becoming rather “regular”
 - Completed: First 4 μ s or past peak current
 - Calculations with $\sim 700,000$ cells complete in less than 48 hours on 64 processors
 - Thermal diffusion stability continues to challenge time stepping and runs past 4 μ s

ALEGRA Input Geometry



Two-Loop Circuit

- Designed from experimental data
- Mesh inductance, resistance calculated by ALEGRA
- Total, mesh, & shunt are defined for current plots



Parameters

$$V_0 = (0.98 * 30.0e+3) \text{ V}$$

$$C_0 = 35.44e-6 \text{ F}$$

$$R_1 = (1.24e-3 - R_A) \Omega$$

$$R_2 = 30.4e-3 \Omega$$

$$R_3 = 3.80e-3 \Omega$$

$$R_A = 0.24e-3 \Omega$$

$$L_1 = (45.03e-9 - L_A) \text{ H}$$

$$L_2 = 519.0e-9 \text{ H}$$

$$L_3 = 30.99e-9 \text{ H}$$

$$L_A = 27.94e-9 \text{ H}$$

ALEGRA Impact to C-EOS (1 of 2)

- Completed simulations of “non-destructive” tests using thicker foil & lower charge voltage
 - Calculated mesh inductance and resistance
 - Accessed accuracy of two-loop circuit model
 - Future work is to calculate current “streamlines” for calibrating magnetic probes

ALEGRA Impact to C-EOS (2 of 3)

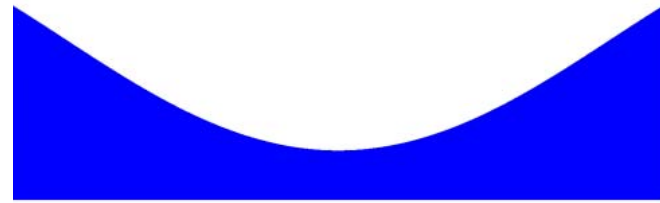
- Completed simulation of destructive test of “legacy” design—constant (straight) width foil
- Simulation showed concerns with “legacy” design
 - Identified initial fuse point away from center at the material “triple point”
 - Diagnostics focused on top and bottom of fuse at center point
 - Physics occurring too late after peak current—laser diagnostics travel through “gem”
 - Material integrity of fused quartz (“gem”) potentially compromised due to shock compression, expansion or fracture
- Concerns warranted a new design—curving the fuse shape with the narrowest width at the center

ALEGRA Impact to C-EOS (3 of 3)

- Halved the width of the fuse at mid-length
 - Curved shape based on polynomial
- Simulations show improved performance
 - Physics occurring sooner and occurring at the point of instrumentation
- Experiment with new shape scheduled for April 2013
- Remaining slides compare performance



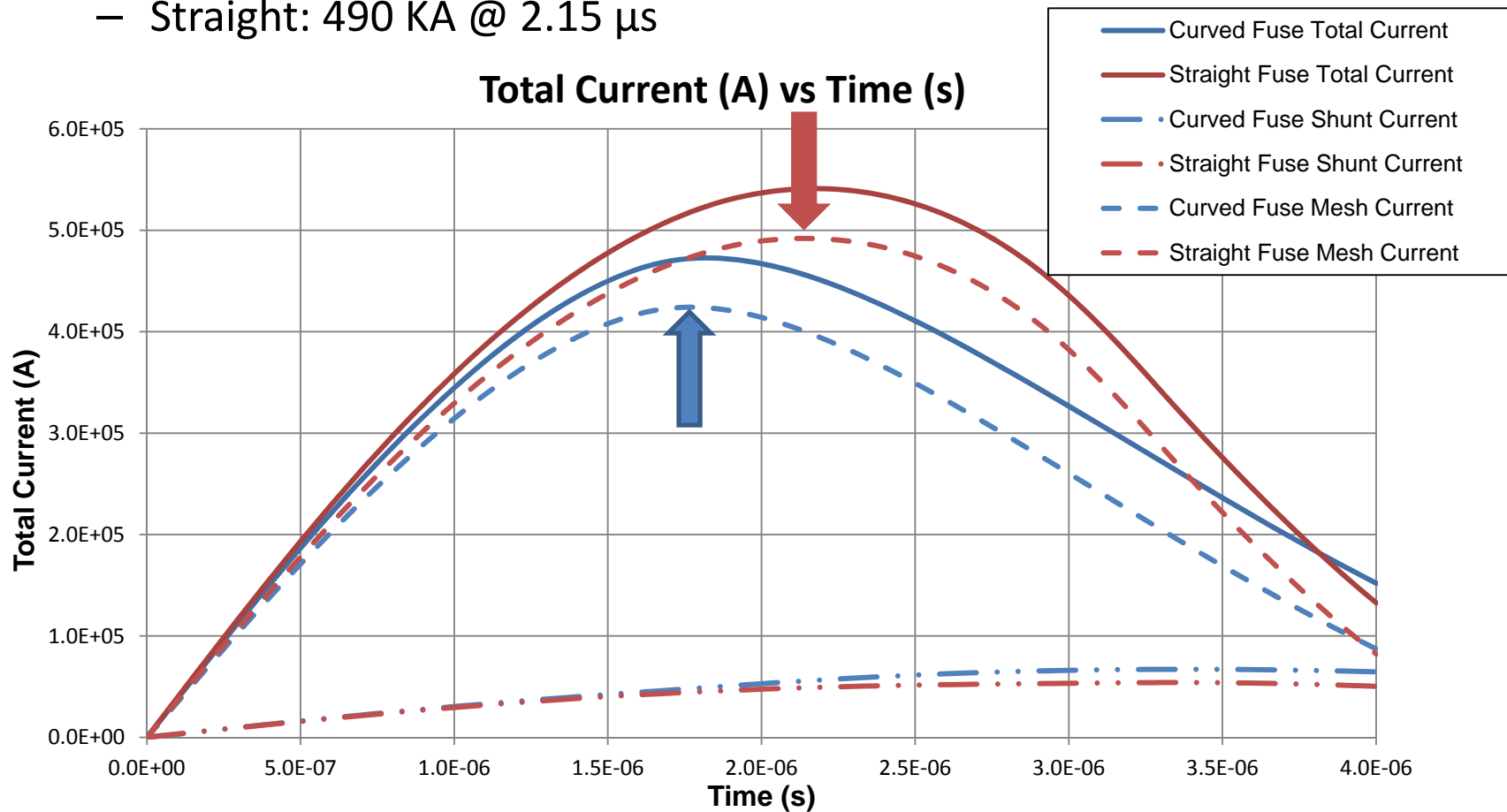
Straight ("Legacy") Shape



Curved Shape

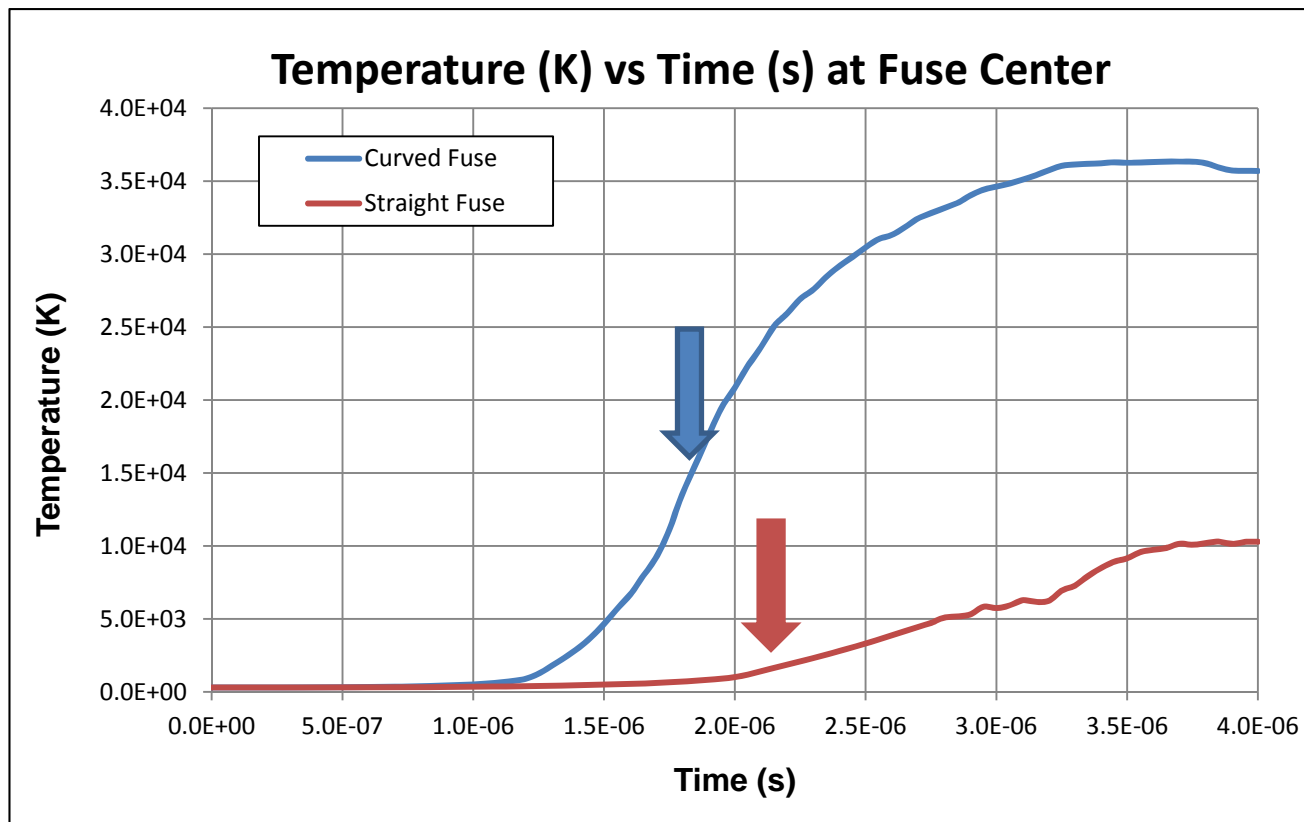
Current Profiles

- Peak Mesh Current (indicated by arrow)
 - Curved: 420 KA @ 1.8 μ s
 - Straight: 490 KA @ 2.15 μ s



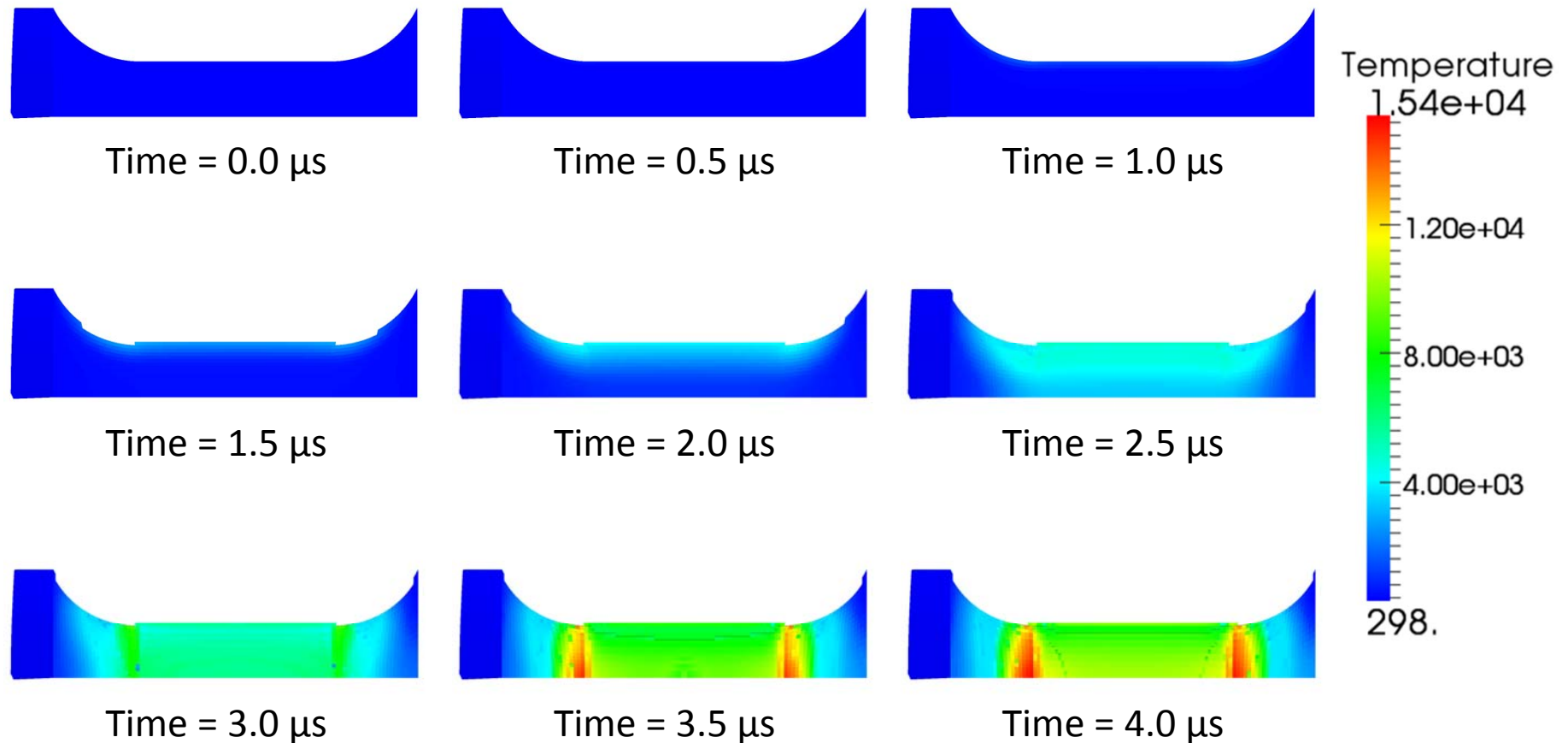
Internal Fuse Temperature at Center

- Temperature at Peak Mesh Current (indicate by arrow)
 - Curved: 1.34 eV or 15,600 °K
 - Straight: 0.15 eV or 1,640 °K



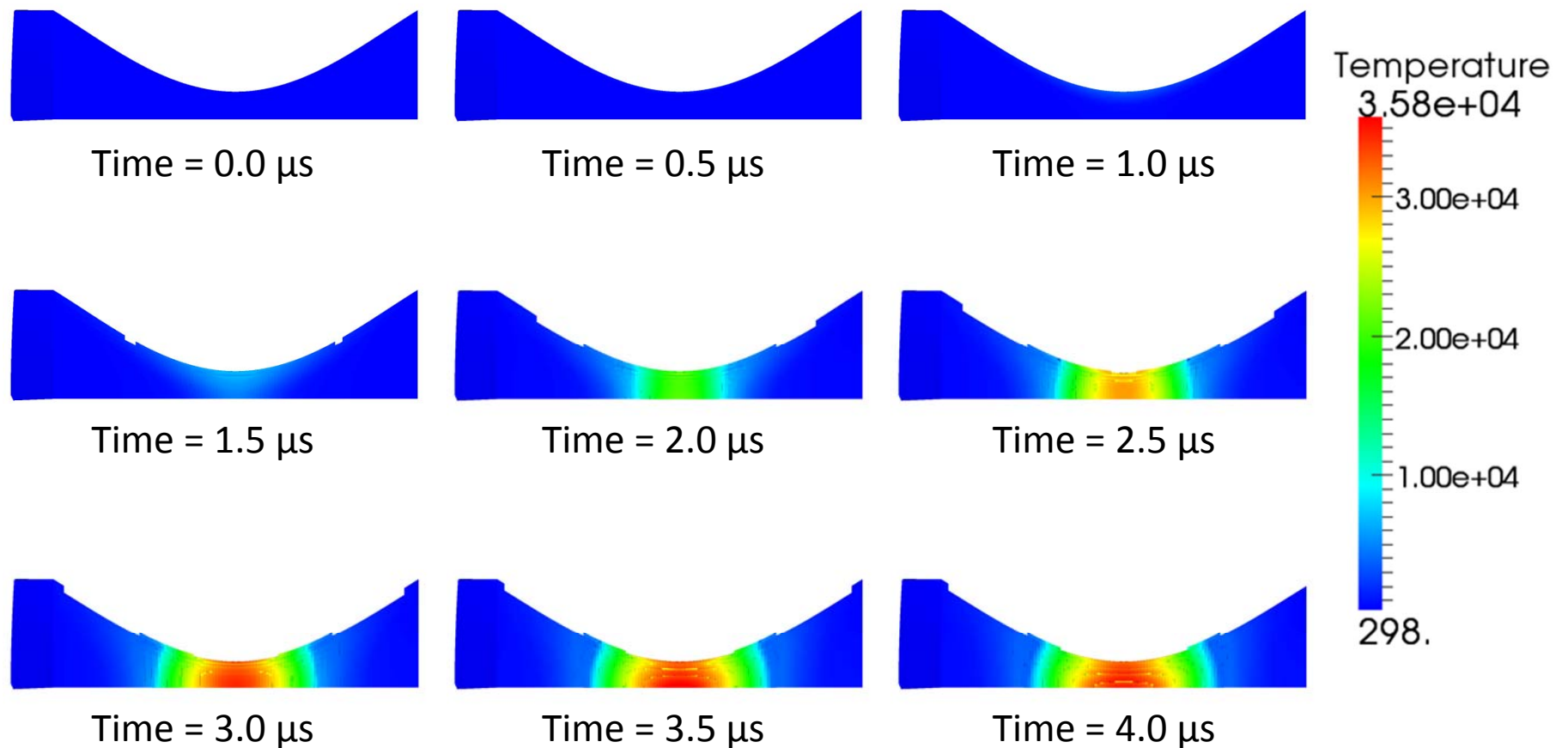
Time History of Fuse Surface Temperature

- Maximum temperature (15,400 °K) at material “triple” point
 - “Triple” point – Fused Quartz (“Gem”), PMMA, and Aluminum



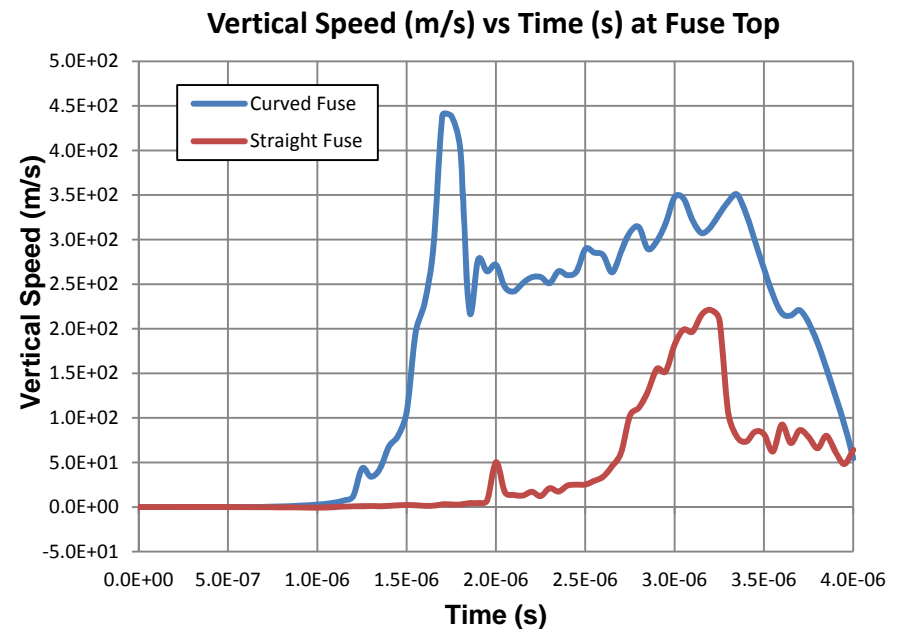
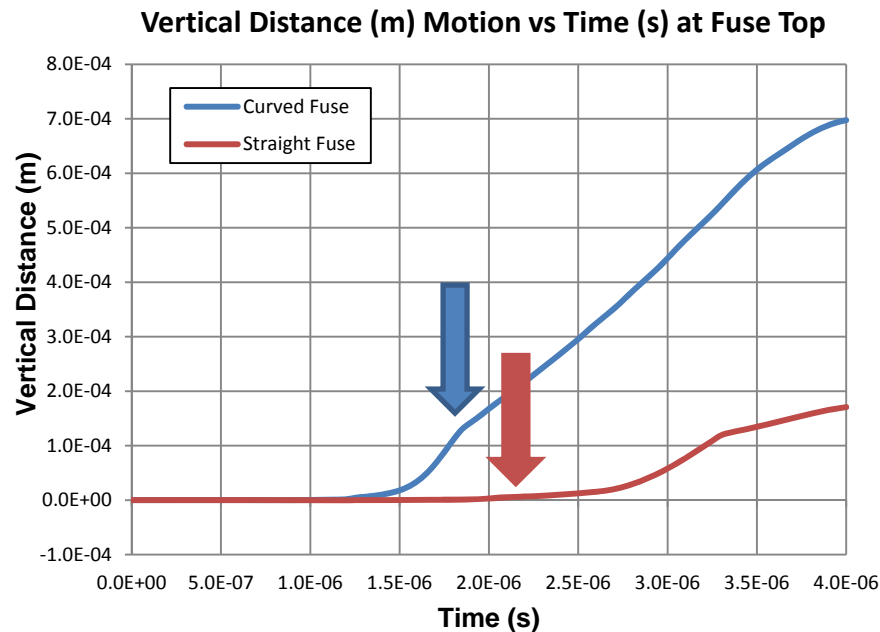
Time History of Fuse Surface Temperature

- Maximum temperature (35,800 °K) at point of measurement



Fuse Dynamics at Top, Center

- Fuse's original thickness was $7.62\text{e-}5$ m
- By $4\text{ }\mu\text{s}$,
 - Curved fuse is 18 times thicker
 - Straight fuse is 4.5 times thicker



Future Work

- C-EOS specific milestones
 - Compare simulation to experimental data
 - Started with current profiles
 - Calculate diagnostic signals
 - Modify material models to improve simulation accuracy
- ALEGRA
 - Increase mesh resolution
 - Exercise diffusion solver to improve computational performance
 - Exercise ALE routines